Contrib Mineral Petrol (1995) 120: 292–310

Ian Cartwright · Julie Vry · Michael Sandiford

Changes in stable isotope ratios of metapelites and marbles during regional metamorphism, Mount Lofty Ranges, South Australia: implications for crustal scale fluid flow

Received 18 April 1994/Accepted: 9 January 1995

Abstract The Mount Lofty Ranges comprises interlayered marbles, metapsammites, and metapelites that underwent regional metamorphism during the Delamarian Orogeny at 470–515 Ma. Peak metamorphic conditions increased from lowermost biotite grade (~ 350–400° C) to migmatite grade (~ 700° C) over 50–55 km parallel to the lithological strike of the rocks. With increasing metamorphic grade, $\delta^{18}O$ values of "normal" metapelites decrease from 14–16‰ to as low as 9.0‰, while $\delta^{18}O$ values of calcite in "normal" marbles decrease from 22–24‰ to as low as 13.2‰. These isotopic changes are far greater than can be accounted for by devolatilisation, implying widespread fluid-rock interaction. Contact metamorphism appears not to have affected the terrain, suggesting that fluid flow occurred during regional metamorphism. Down-temperature fluid flow from synmetamorphic granite plutons ($\delta^{18}O = 8.4$–8.6‰) that occur at the highest metamorphic grades is unlikely to explain the resetting of oxygen isotopes because: (a) there is a paucity of skarns at granite-metasediment contacts; (b) the marbles generally do not contain low-XCO_2 mineral assemblages; (c) there is insufficient granite to provide the required volumes of water; (d) the marbles and metapelites retain a several permil difference in $\delta^{18}O$ values, even at high metamorphic grades. The oxygen isotope resetting may be accounted for by along-strike up-temperature fluid flow during regional metamorphism with time-integrated fluid fluxes of up to 5×10^9 moles/m^2 ($\sim 10^5$ m^3/m^2). If fluid flow occurred over 10^5–10^6 years, estimated intrinsic permeabilities are 10^{-20} to 10^{-16}m^2. Variations in $\delta^{18}O$ at individual outcrops suggest that time-integrated fluid fluxes and intrinsic permeabilities may locally have varied by at least an order of magnitude. A general increase in XCO_2 values of marble assemblages with metamorphic grade is also consistent with the up-temperature fluid-flow model. Fluids in the metapelites may have been derived from these rocks by devolatilisation at low metamorphic grades; however, fluids in the marbles were probably derived in part from the surrounding siliceous rocks. The marble-metapelite boundaries preserve steep gradients in both $\delta^{18}O$ and XCO_2 values, suggesting that across-strike fluid fluxes were much lower than those parallel to strike. Up-temperature fluid flow may also have formed orthoamphibole rocks and caused melting of the metapelites at high grades.

This paper is a contribution to IGCP Project 304 "Lower Crustal Processes"

I. Cartwright (✉) · J. Vry
Victorian Institute of Earth and Planetary Sciences, Department of Earth Sciences, Monash University, Clayton Vic 3168, Australia

M. Sandiford
Department of Geology and Geophysics, University of Adelaide, GPO Box 498, Adelaide SA 5001, Australia

Editorial responsibility: R. Binns

Introduction

Constraining crustal fluid flow is very important in understanding tectonometamorphic processes. If fluids are present in significant volumes during metamorphism they may control the stability of mineral assemblages, transport heat and mass, and influence deformation. Fluid flow in metamorphic terrains may occur isothermally or along temperature gradients. Up- and down-temperature fluid flow will potentially produce distinctly different patterns of isotopic and mineralogical resetting (Baumgartner and Ferry 1991; Dipple and Ferry 1992a; Ferry 1994) that theoretically can be used to determine the direction of fluid flow. Down-temperature fluid flow that drives devolatilisation reactions in calcareous or pelitic rocks under equilibrium conditions is predicted to produce zones of high-variance mineral assemblages separated by relatively sharp reaction fronts. By contrast, as long as the volumes of fluid

do not overwhelm the buffering capacity of the rock, up-temperature fluid flow may result in the widespread formation of mineral assemblages that are isobarically univariant in the simple end-member systems. If isotopic equilibrium is maintained, up-temperature fluid flow will generally lower $\delta^{18}O$ values at high temperatures due to the temperature dependence of the fluid-rock partition coefficients for ^{18}O. Up-temperature fluid flow may also cause depletion of some major elements (e.g. Si and K) due to the increased solubility of these elements with increasing temperature (Dipple and Ferry 1992b), while down-temperature fluid flow is predicted to cause enrichment of these elements. However, the predicted mineralogical, isotopic, and geochemical changes are based on the results of one-dimensional, steady state, equilibrium fluid-flow models. If there is incomplete exchange between the fluid and the rock, fluid channelling leading to transverse dispersion, or significant kinematic dispersion during fluid flow, simple discriminants of the direction of fluid flow may not apply (e.g. Huang and Bowman 1993; Bowman et al. 1994; Cartwright 1994; Cartwright and Oliver 1995). Therefore, it is necessary to consider several lines of geochemical and petrological evidence to constrain the direction of fluid flow.

Changes in stable isotope ratios during regional metamorphism

Unmetamorphosed sediments usually have characteristic $\delta^{18}O$ values (e.g. Hoefs 1980). In general, limestones have the highest $\delta^{18}O$ values (20–30‰), followed by shales (15–20‰), and quartzites (10–15‰). Metasediments in some metamorphic terrains have $\delta^{18}O$ values that are similar to those of their unmetamorphosed equivalents (e.g. calc-silicates in the Mary Kathleen Fold Belt, Australia, Cartwright 1994; marbles in the Adirondacks, USA, Valley et al. 1990; greywackes in the Franciscan terrain, USA, Margaritz and Taylor 1976; and quartzites in New Hampshire, USA, Rumble 1978). In addition, metasediments from the KTB (Continental Deep Bore) drill hole, Germany, show only a slight decrease in $\delta^{18}O$ values from rocks metamorphosed at 150° C (~ 11–13‰) to those metamorphosed at 400° C (~ 9–12‰), which may be due to devolatilisation without significant fluid infiltration (Simon and Hoefs 1993).

Relatively large shifts in $\delta^{18}O$ values are, however, documented from metasediments in some regional metamorphic terrains. For example, marbles and metapelites from high-grade areas of the Northern Great Basin, USA, have $\delta^{18}O$ values that are up to 5–10‰ lower than their low-grade equivalents (Wickham 1990). Granulite facies calcareous and pelitic metasediments in the Lewisian complex, UK, have $\delta^{18}O$ values of 8–10‰ (Cartwright and Valley 1992). The $\delta^{18}O$ values of siliceous and pelitic gneisses in the Ryoke belt, Japan, decrease from 24 to 13‰ and 18 to 13‰, respectively from biotite to migmatite grade (Honma and Sakai 1975). Hence, $\delta^{18}O$ values of sedimentary rocks are sometimes, but not universally, lowered by several permil during regional metamorphism. The $\delta^{18}O$ values are probably lowered by < 1–2‰ by prograde metamorphic devolatilisation (e.g. Chamberlain et al. 1990; Stern et al. 1992), suggesting that closed system reactions are not the major cause of isotopic resetting. This assertion is supported by the fact that rocks in some metamorphic terrains that have undergone prograde devolatilisation retain little-reset oxygen isotope values. It is most likely that, as in contact metamorphism (Valley 1986; Nabelek 1991), the lowering of $\delta^{18}O$ values by several permil during regional metamorphism reflects fluid infiltration.

While documenting the lowering of $\delta^{18}O$ values during regional metamorphism is important in understanding crustal fluid flow, there are few terrains where progressive isotopic changes can be studied. Here, we document the progressive changes of stable isotope ratios and mineralogy of 71 marble and 156 metapelite samples from the Mount Lofty Ranges, South Australia (Fig. 1), and use these data to characterise regional metamorphic fluid flow. The Mount Lofty Ranges is an ideal terrain in which to study large scale isotopic changes, because: (1) a coherent stratigraphy exists from low to high metamorphic grades, including tens-of-metre thick marble layers that act as marker units; (2) the area has a relatively simple structural and metamorphic history; (3) a wide range of rock types exists allowing fluid flow in different units to be compared; (4) there is a paucity of veins or mineralised faults suggesting that local fluid-flow was not superimposed on any regional-scale fluid-flow systems.

Analytical techniques

Stable isotope ratios were measured at Monash University. Oxygen isotope ratios of silicates were analysed following Clayton and Mayeda (1963) using ClF_3 as the oxidising reagent and CO_2 was extracted from calcite by reaction with H_3PO_4 at 25° C for 12–18 hours (McCrea 1950). Extracted gases were analysed as CO_2 on Finnigan MAT Delta-E and 252 mass spectrometers and the results are expressed relative to PDB (Peedee belemnite; carbon) and V-SMOW (Standard mean ocean water; oxygen). Internal and international standards run at the same time as the samples in this study generally yielded values within ± 0.2‰ of their accepted values. Mineral compositions used to estimate *P-T* conditions (Table 3) were determined on a Cameca Camebax SX50 electron microprobe at the University of Melbourne and an ARL SEMQ2 electron microprobe at Monash University.

Local geology

The Mount Lofty Ranges is part of the Palaeozoic Adelaide Fold Belt and contains rocks of the Kanmantoo group, which are a sequence of metasandstones, metapelites, and metasiltstones with

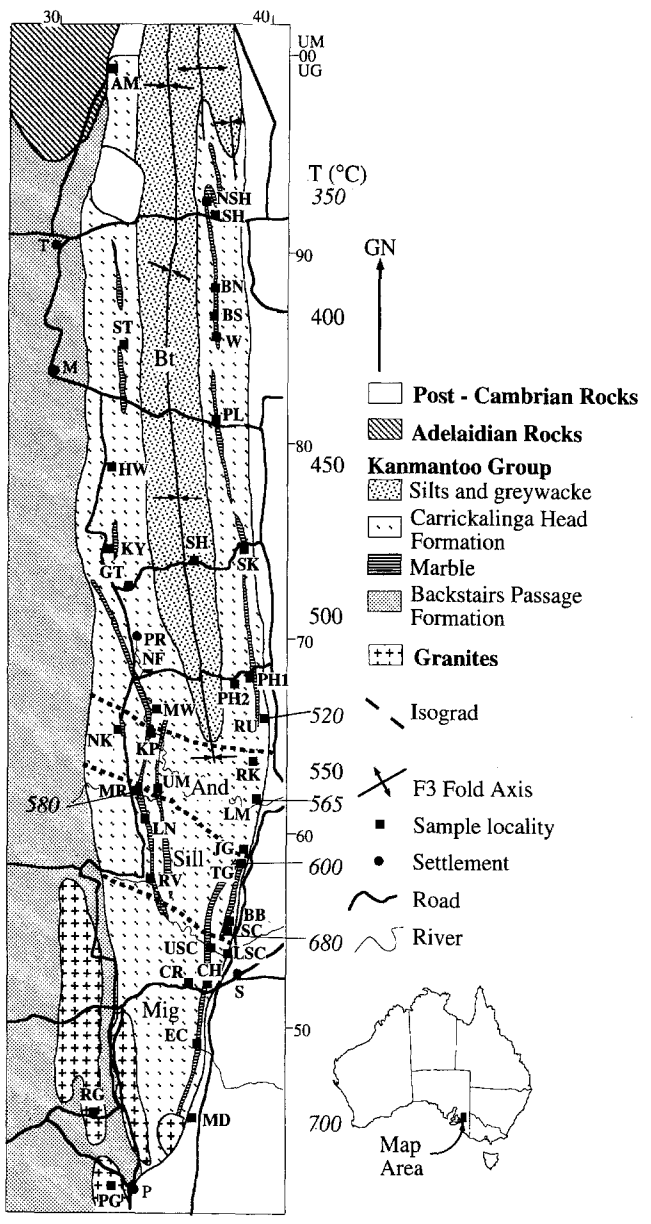

Fig. 1 Geological map of the Mount Lofty Ranges (after Offler and Fleming 1968; Sandiford et al. 1990; and Dymoke and Sandiford 1992). *Dotted lines* separate the main metamorphic zones, (*Bt* biotite zone; *And* andalusite-staurolite zone, *Sill* sillimanite-fibrolite zone, *Mig* migmatite zone). Temperatures indicate approximate peak metamorphic temperatures (numbers in *italics* are discussed in the text). Sample localities are listed in Tables 1 and 2. Settlements *P* Palmer, *S* Sanderston, *M* Moculta, *T* Truro. *Tick marks* show the gridlines on the Australian Map Grid, the area is on the Tepko (6728-3), Angaston (6728-4), and Truro (6729-3) 1:50,000 map sheets published by the Geological Survey of South Australia, Adelaide, Australia

minor carbonates (Fig. 1). The terrain was metamorphosed in the Delamarian Orogeny at 470–515 Ma, and there is a regular increase in peak metamorphic grade from lowermost biotite zone in the north through andalusite-staurolite, fibrolite, and sillimanite zones to migmatite zone in the south (Sandiford et al. 1990; Dymoke and Sandiford 1992; Fig. 1). Polyphase deformation during the Delamarian orogeny culminated in the production of kilometre-scale D2 upright folds that were formed close to the peak of metamorphism, and which control the outcrop pattern. A north–south trending, steeply dipping, S2 foliation is apparent through much of the terrain. The granites in the high-grade regions of the terrain were emplaced close to the thermal peak of metamorphism (Foden et al. 1990), and small metre-wide cross-cutting granite sheets are locally present in the migmatite, sillimanite, and fibrolite zones.

Petrology of marbles and metapelites

The petrology of the metapelites is summarised in Table 1 (sample locations on Fig. 1). At the lowest metamorphic grades, the rocks comprise quartz + chlorite + muscovite + plagioclase assemblages with biotite that is, in general, poorly formed. With increasing temperature, biotite becomes more prominent and chlorite disappears. In the andalusite-staurolite zone, the rocks commonly contain combinations of andalusite, staurolite, cordierite, and garnet. At higher grades (fibrolite, sillimanite, and migmatite zones), fibrolite then prismatic sillimanite appear at the expense of andalusite and staurolite (Sandiford et al. 1990; Dymoke and Sandiford 1992). At the highest metamorphic grades, cordierite, garnet, and sillimanite may be present and the rocks show the development of migmatitic textures that have been interpreted as resulting from *in situ* partial melting (Offler and Flemming 1968). Locally in the fibrolite zone, and generally in the sillimanite and migmatite zones, K-feldspar replaces muscovite as a peak metamorphic phase; although texturally late muscovite is often observed. The highest-grade minerals in most rocks are aligned in the regional S2 foliation. Andalusites contain curved and crenulated inclusion trails that indicate that andalusite either grew during progressive D2 deformation or overgrew an earlier fabric. While minor retrogression of some metapelites is indicated by the growth of muscovite, or more rarely chlorite, at an angle to the D2 fabrics or the partial pinnitisation of cordierite (Table 1), the pelitic rocks have generally not undergone extensive retrogression. Late orthoamphibole, usually with cordierite, is present at several localities in the staurolite-andalusite or fibrolite zones (Table 1). Arnold and Sandiford (1990) show that the formation of orthoamphibole involved the breakdown of biotite without formation of another K_2O-bearing mineral. These authors conclude that K_2O was removed from the rocks during fluid infiltration.

The petrology of the marbles is summarised in Table 2 (locations in Fig. 1). The marbles at lowest metamorphic grades contain calcite + quartz ± K-feldspar ± plagioclase ± talc. With increasing grade muscovite, phlogopite, tremolitic amphibole, and diopside appear (Table 2). K-feldspar is absent in the middle of the terrain but reappears at higher grades and scapolite is present in some marbles at high grades. Marbles directly adjacent to the Milendella granite (MD, Fig. 1) contain garnet + wollastonite. Samples at the edge of the marble layer in Trough Gully are spinel bearing. An isolated occurrence of vesuvianite marble (not sampled in this study) occurs at the edge of the marble layer near Jo's Gully, and marbles from the margins of the layer in Lower Saunders Creek contain late clinozoisite. However, aside from these rare occurrences that are all from marbles within 5 m of the adjacent pelites or granites, the marbles do not generally contain the low-X_{CO_2} assemblages that characterise marbles which have been infiltrated by water-rich fluids (e.g. Tracy and Frost 1991).

Metamorphic temperature gradient and marble X_{CO_2} values

As shown by Fig. 1 the rocks in the Mount Lofty Ranges record peak metamorphic conditions from lowermost biotite to migmatite grade. Estimated *P-T* conditions are shown in Table 3. The pressures and temperatures of the lowest-grade assemblages are the

Table 1 Mineralogy and oxygen isotope ratios of granites and metapelites from the Mount Lofty Ranges (Abbreviations: *And* andalusite, *Ap* apatite, *Bt* biotite, *Cc* calcite, *Chl* chlorite, *Crd* cordierite, *Gnt* garnet, *Hbl* hornblende; *Ksp* K-feldspar, *Mt* magnetite, *Mus* muscovite, *O-Amp* orthoamphibole, *Plg* plagioclase, *Py* pyrite, *Qtz* quartz, *Sill* sillimanite, *Tour* tourmaline, *Zir* zircon, *WR* whole rock; *X* peak metamorphic mineral, *L* major late mineral (> 5%), *l* minor late mineral (< 5%), *R* retrogressed, *f* fibrolite, *s* sericitized, *p* poorly formed)

Granites		$\delta^{18}O$[a]										
Sample	Location[c]	WR	Qtz	Bt	Qtz	Bt	Mus	Plg	Ksp	Mt	Zir	
V93-65	Palmer Granite (PG)	8.5	9.5	5.0	X	X	l	X	X	X	X	
V93-63	Rathjen Gneiss (RG)	8.6	9.9	5.1	X	X	l	X	X		X	
V93-64	Rathjen Gneiss (RG)	8.4	10.1	4.9	X	X	l	X	X	X	X	
Average			8.5 ± 0.1									

Metapelites																
Sample	Location	Dist[b]	$\delta^{18}O$	Qtz	Bt	Mus	Chl	Plg	Ksp	And	Sill	Crd	Gnt	O-Amp	Other	Melt
Migmatite Zone																
V92-37	Milendella (MD)	0.0	10.6[d]	X	X, R	l	l		X(s)		L(f)	R			Mt L, Zir X	X
V92-38	Milendella (MD)	0.0	11.3	X	X	l		X	X						Tour X, Zir X	
V92-39	Milendella (MD)	0.0	10.5	X	X, R	L	l		X(s)		L(f)	R			Mt L, Zir X	X
V92-111	Emu Creek (EC)	3.1	13.7	X	X	l		X	X						Ap X	X
V92-112	Emu Creek (EC)	3.1	9.5	X				X	X						Hbl X	
V92-113	Emu Creek (EC)	3.1	10.7	X	X, R	l		X	X						Tour, X	
V92-116	Emu Creek (EC)	3.1	10.0	X	X			X	X						Mt X	
V92-118	Cooke Hill Rd (CR)	6.3	11.1	X	X			X	X						Mt X, Py X	
V92-119	Cooke Hill Rd (CR)	6.3	12.9	X	X	l		X	X						Zir X	
V92-120	Cooke Hill (CH)	6.8	10.9	X	X	l		X	X						Ap X, Zir X	X
V92-121	Cooke Hill (CH)	6.8	11.0	X	X	L		X	X			R			Mt X, Zir X	
V92-122	Cooke Hill (CH)	6.8	9.8	X	X	L		X	X		L(f)	R			Zir X	
V92-129	Cooke Hill (CH)	6.8	9.7	X	X	L		X	X			R			Zir X	
V92-130	Cooke Hill (CH)	6.8	9.9	X	X	L		X	X		L(f)	R			Ap X, Mt X	
V92-131	Cooke Hill (CH)	6.8	10.5	X	X	L		X	X			R			Zir X	
V92-1	Lower Saunders CK (LSC)	8.0	*10.1*	X	X			X						L	Mt X	
V92-4	Lower Saunders CK (LSC)	8.0	*10.6*	X	R			X	X			X(p)		L	Zir X	
V92-5	Lower Saunders CK (LSC)	8.0	10.2	X	X		L	X	X			X(p)	R		Ap X, Mt X	
V92-7	Lower Saunders CK (LSC)	8.0	9.6	X	X	L		X	X			X(p)			Zir X	X
V92-8	Lower Saunders CK (LSC)	8.0	9.5	X	X		l	X	X			X(p)	X, r		Mt X, l ,Zir X	X
V92-10	Lower Saunders CK (LSC)	8.0	9.8	X	X		L	X	X			X(p)	R		Mt l	
V92-11	Lower Saunders CK (LSC)	8.0	11.1	X	X,L	l	l	X	X						Ap X, Mt l, Zir X	
V92-12	Lower Saunders CK (LSC)	8.0	10.8	X	X	l	l	X	X		X(f)	X(p)			Mt X	X
V92-13	Lower Saunders CK (LSC)	8.0	11.1	X	X		L	X(s)	X(s)						Cc X, Zir X	
V92-23	Lower Saunders CK (LSC)	8.0	11.8	X	X	l	l	X	X						Zir X	
V92-24	Lower Saunders CK (LSC)	8.0	11.8	X	X	l	l	X	X						Ap X, Mt X, Zir X	
V93-25	Lower Saunders CK (LSC)	8.0	9.3	X	X	l	L	X(s)	X(s)			X(p)			Tour X	
V92-31	Upper Saunders CK (USC)	8.6	**12.8**	X	X	l		X	X		L(f)	X, R			Tour X, Zir X	
V92-32	Upper Saunders CK (USC)	8.6	**13.5**	X	X	l		X	L(f)		R				Tour X	
V92-33	Upper Saunders CK (USC)	8.6	9.0	X	X	l		X	X						Ap X, Tour X	
Average			10.5 ± 0.9													
Sillimanite zone																
V92-154	Saunders Camp (SC)	8.7	10.7	X	X	l		X	X		L(f)	X, R			Ap X, Zir X	
V92-156	Saunders Camp (SC)	8.7	11.5	X	X	L						R			Ap X, Mnt	
V92-157	Saunders Camp (SC)	8.7	10.4	X	X			X	X						Tour X	
V92-158	Saunders Camp (SC)	8.7	10.5	X	X	l			X		L(f)	R			Zir X	
V92-92	Bernburra (BB)	9.3	*10.3*	X	X, R			X					X	L	Mt L	
V92-94	Bernburra (BB)	9.3	*9.9*	X	X	l		X	X					L		
V92-96	Bernburra (BB)	9.3	10.1	X	X	L	l	X	X		L(f)		R		Zir X	
V92-97	Bernburra (BB)	9.3	10.0	X	X	L		X	X			R			Ap X, Zir X	
V92-98	Bernburra (BB)	9.3	10.1	X	X			X	X			X(p)	X			
V92-99	Bernburra (BB)	9.3	10.5	X	X	L		X	X			R			Ap X, Zir	
V92-100	Bernburra (BB)	9.3	11.2	X	X	L		X							Mt X	
V92-101	Bernburra (BB)	9.3	10.4	X	X			X	X						Mt X, Zir X	?X
V92-102	Bernburra (BB)	9.3	11.0	X	X	L		X	X(s)		L(f)	R			Mt X, Zir X	
V92-105	Bernburra (BB)	9.3	11.4	X	X			X	X						Zir X	
V92-106	Bernburra (BB)	9.3	10.9	X	X	L	l	X	X		L(f)	R			Ap X	
V92-107	Bernburra (BB)	9.3	10.9	X	X	L		X	X		L(f)	R			Mt X	
V93-61	Rishmin Valley (RV)	11.7	10.4	X	X	l		X	X		L(f)				Mt X	
V93-62	Rishmin Valley (RV)	11.7	11.1	X	X	l		X	X		L(f)				Ap X, Mt X	
V92-61	Trough Gully (TG)	13.0	13.4	X	X	L		X	X		L(f)	R			Tour X	
V92-62	Trough Gully (TG)	13.0	13.0	X	X	L					L(f)	R			Ap X	
V92-63	Trough Gully (TG)	13.0	13.0	X	X	L		X	X		L(f)	R			Mt X, Tour X	
V92-69a	Trough Gully (TG)	13.0	11.1	X	X	X									Mt X, Zir X	

Table 1 (continued)

Sample	Location	Dist[b]	$\delta^{18}O$	Qtz	Bt	Mus	Chl	Plg	Ksp	And	Sill	Crd	Gnt	O-Amp	Other	Melt
V92-69b	Trough Gully (TG)	13.0	11.9	X	X	X		X							Mt X, Zir X	
V92-76	Trough Gully (TG)	13.0	10.7	X	X	L			X		L(f)	R			Ap X	
V92-77	Trough Gully (TG)	13.0	10.5	X	X	L		X	X		L(f)	R			Ap X, Zir X	
V92-78	Trough Gully (TG)	13.0	10.5	X	X	L		X	X		L(f)	R				
V92-84	Jo's Gully (JG)	13.6	10.9	X	X	l		X	X		L(f)	R			Ap X, Zir X	
V92-86	Jo's Gully (JG)	13.6	*10.6*	X	X, R	l	l	X						L		
V92-87	Jo's Gully (JG)	13.6	11.0	X	X			X	X						Zir X	
V92-88	Jo's Gully (JG)	13.6	10.9	X	X			X	X							
V92-89	Jo's Gully (JG)	13.6	*10.4*	X	X	l		X						L	Zir X	
V93-15	Jo's Gully (JG)	13.6	9.5	X	X	l		X				X			Sta R, Ilm X	
V93-56	Lessen North (LN)	14.3	9.9	X	X	l		X	X				X		Ap X, Mt X, Zir X	
V93-57	Lessen North (LN)	14.3	10.0	X	X	l		X	X				X		Ap X, Mt X, Zir X	
V92-58	Marne Reserve (MR)	14.8	10.8	X	X	l		X	X				X		Hem X, Tour X	
V92-59	Marne Reserve (MR)	14.8	11.2	X	X	l			X				X		Ap X, Mt X, Zir X	
V92-199	Marne Reserve (MR)	14.8	**14.6**	X	X	X, L		X							AP X	
V92-200	Marne Reserve (MR)	14.8	**14.0**	X	X	X, L		X	X							
V92-201	Marne Reserve (MR)	14.8	**12.0**	X	X	L		X							Mt X	
V92-202	Marne Reserve (MR)	14.8	**11.3**	X	X	l		X							Sta X	
V93-13	Marne Reserve (MR)	14.8	*8.3*	X	X, R			X						X	Mt X	
V93-14	Marne Reserve (MR)	14.8	*8.4*	X	X, R			X						X	Mt X	
Average			11.0 ± 0.9													
Andalusite-staurolite zone																
V92-190	Upper Marne (UM)	15.3	11.1	X	X	L	l	X	X						Mt X	
V92-192	Upper Marne (UM)	15.3	11.5	X	X	X, L		X	X				X		Ap X, MtX, Tour	
V92-195	Upper Marne (UM)	15.3	11.3	X	X	X									Tour X	
V92-196	Upper Marne (UM)	15.3	11.9	X	X	X, L	l									
V92-197	Upper Marne (UM)	15.3	11.0	X	X			X							Tour X	
V92-132	Lower Marne (LM)	15.6	*11.5*	X	X		l	X						X	Ap X	
V93-133	Lower Marne (LM)	15.6	11.8	X	X	L			X						Mt X	
V92-137	Lower Marne (LM)	15.6	9.4	X	X	X,L	l	X				R			Mt X, Zir X	
V92-138	Lower Marne (LM)	15.6	11.1	X	X	L	L	X		X		R			Sta L, Zir X	
V92-140	Lower Marne (LM)	15.6	9.6	X	X	X,L	L	X				R			Mt X, Zir X	
V92-141	Lower Marne (LM)	15.6	11.2	X	X	X,L		X	X	X		R				
V92-142	Lower Marne (LM)	15.6	10.1	X	X	X,L	l					R			Ap X, Zir X	
V92-143	Lower Marne (LM)	15.6	11.6	X	X	l		X	X			X,R	L		Zir X	
V92-144	Lower Marne (LM)	15.6	11.7	X	X	X,L		X		X					Zir X	
V92-145	Lower Marne (LM)	15.6	12.1	X	X	L			X	X					Zir X	
V92-147	Lower Marne (LM)	15.6	12.5	X	X	X,L		X		X	L(f)	R			Zir X, Mt L	
V92-148	Lower Marne (LM)	15.6	12.2	X	X	X,L		X		X	L(f)				Sta L?	
V92-149	Lower Marne (LM)	15.6	12.1	X	X	X,L				X	L(f)				Sta L?	
V92-150	Lower Marne (LM)	15.6	12.9	X	X	L		X				R				
V92-160	Rocky Creek (RK)	18.1	12.1	X	X	X,L				X	L(f)				Sta L?	
V92-161	Rocky Creek (RK)	18.1	12.8	X	X	X		X		X	L(f)		X		Mt X, Zir X	
V92-162	Rocky Creek (RK)	18.1	11.3	X	X	X				X			X		Mt X	
V92-163	Rocky Creek (RK)	18.1	13.8	X	X	X		X							Tour X, Mt X, Zir X	
V92-164	Rocky Creek (RK)	18.1	11.8	X	X	X		X		X	L(f)		X		Mt X, Zir X	
V92-166	Rocky Creek (RK)	18.1	11.1	X	X	X,L			X, R				X			
V92-167	Rocky Creek (RK)	18.1	12.0	X	X	l		X			L(f)	R			Zir X	
V92-168	Rocky Creek (RK)	18.1	11.6	X	X	X,L				X					Zir X	
V92-169	Rocky Creek (RK)	18.1	12.2	X	X	X,L				X					Zir X	
V92-170	Rocky Creek (RK)	18.1	12.9	X	X	X,L				X					Ap X, Zir X	
V92-171	Rocky Creek (RK)	18.1	10.8	X	X	L						X		L	Zir X	
V92-172	Rocky Creek (RK)	18.1	13.0	X	X	X						X			Zir X	
V92-174	Rocky Creek (RK)	18.1	13.8	X	X	X		X							Tour X, Zir X	
V92-175	Rocky Creek (RK)	18.1	13.2	X	X	X						X			Zir X	
V92-57	Nunkuri (NK)	18.8	10.8	X	X	X		X		X					Ap X, Sta	
Average			11.8 ± 1.1													
Biotite zone																
V92-151	Kappalunta (KP)	19.1	13.2	X	X	X,L		X					X		Ap X, Mt X,	
V93-54	M Wrights Road (MW)	19.7	12.4													
V93-55	M Wrights Road (MW)	19.7	12.2													
V92-183	Ruin (RU)	20.0	12.7	X	X	X,L									Ap X, Tour X	
V92-185	Ruin (RU)	20.0	12.0	X	X		l	X	?					L	Sph X	

Table 1 (continued)

Sample	Location	Dist[b]	$\delta^{18}O$	Qtz	Bt	Mus	Chl	Plg	Kps	And	Sill	Crd	Gnt	O-Amp	Other	Melt
V92-186	Ruin (RU)	20.0	11.9	X	X			X						L	Mt X, Sph X	
V92-187	Ruin (RU)	20.0	12.9	X	X	X,L		X							Ap X	
V92-189	Ruin (RU)	20.0	11.9	X	X	X,L									Tour X	
V92-52	Pine Hut Rd 2 (PH2)	22.1	12.7	X	X	X	X								Mt X, Tour X	
V92-53	Pine Hut Rd 2 (PH2)	22.1	11.4	X	X	X	X	X							Ap X, Tour X	
V92-55	Pine Hut Rd 2 (PH2)	22.1	12.0	X	X	X	X								Ap X, Tour X	
V92-153	Netherford (NF)	22.3	10.9	X	X	X,L		X							Mt X, Tour X	
V93-52	Netherford (NF)	22.3	10.8	X	X	X		X							Ap X, Tour X	
V92-176	Pine Hut Road 1 (PH1)	22.3	11.9	X	X	X	l	X							Tour X, Mnt X	
V92-177	Pine Hut Road 1 (PH1)	22.3	12.0	X	X	X	X	X							Tour X, Mt X, Zir X	
V92-178	Pine Hut Road 1 (PH1)	22.3	12.2	X	X	X									Mt X, Tour X	
V92-178	Pine Hut Road 1 (PH1)	22.3	11.5	X	X	X		X							Mt X, Tour X	
V92-180	Pine Hut Road 1 (PH1)	22.3	11.9	X	X	X,L	X								Mt X, Cc X	
V92-181	Pine Hut Road 1 (PH1)	22.3	11.7	X	X	X		X							Zir X	
V92-182	Pine Hut Road 1 (PH1)	22.3	12.7	X	X	X	X	X							Mt X	
V93-5	Pine Hut Road 1 (PH1)	22.3	*10.8*	X	X	X		X							Tour X	
V93-6	Pine Hut Road 1 (PH1)	22.3	11.2	X	X	X		X							Ap X, Mt X	
V92-51	Prongorong (PR)	24.0	15.0	X	X	X	l	X							Ap X	
V93-47	Graetz Town (GT)	26.8	10.9	X	X	X	l	X								
V93-48	Graetz Town (GT)	26.8	11.3	X	X	X		X							Mt X	
V93-49	Graetz Town (GT)	26.8	11.2	X	X	X	X								Tour X	
V92-51	Sedan Hill (SH)	28.3	14.4	X	X	X	X								Mt X, Tour X	
V92-47	Sedan Road (SR)	29.1	13.0	X	X	X	X	X							Cc X, Tour X	
V92-48	Sedan Road (SR)	29.1	15.0	X	X	X	X	X							Mt X	
V92-49	Sedan Road (SR)	29.1	12.4	X	X	X	X	X							Ap X, Tour X, Mt X	
V92-50	Sedan Road (SR)	29.1	12.7	X	X	X	X	X							Mt X, Tour X	
V93-43	Henschke Winery (HW)	34.2	13.3	X	X	X	l	X							Ap X	
V93-44	Henschke Winery (HW)	34.2	13.6	X	X	X	X	X								
V93-40	Pipeline (PL)	35.5	12.7	X	X	X		X							Mt X	
V93-41	Pipeline (PL)	35.5	13.2	X	X	X		X							Tour X	
V93-42	Pipeline (PL)	35.5	12.6	X	X	X	X								Mt X, Tour X	
V93-34	Standish (ST)	38.4	13.6	X	X	X	X								Tour X	
V93-35	Standish (ST)	38.4	14.0	X	X	X	X	X							Tour X	
V93-31	Wyeroo (W)	38.6	13.0	X	X	X	X	X							Ap X, Tour, Mt X	
V93-29	Baldon South (BS)	39.8	12.1	X	X	X	X								Ap X, Mt X	
V93-30	Baldon South (BS)	39.8	13.9	X	X	X	X	X							Mt X, Tour X	
V93-22	Baldon North (BN)	41.3	12.7	X	X	X	X	X								
V93-23	Baldon North (BN)	41.3	14.2	X	X	X	X	X							Tour X	
V93-26	Baldon North (BN)	41.3	14.8	X	X	X	X	X							Mt X, Tour X	
V92-44	Sturt Highway (SH)	45.5	14.3	X	X(ρ)	X,l	X	X							Tour X, Mt X	
V92-45	Sturt Highway (SH)	45.5	15.3	X	X(ρ)	X,l	X	X							Ap X, Tour X, Mt X	
V93-18	Sturt Highway (SH)	45.5	14.7	X	X(ρ)	X,l	X	X							Tour X	
V93-19	Sturt Highway (SH)	45.5	15.5	X	X(ρ)	X,l	X	X							Tour X	
V93-36	Ameroo (AM)	53.2	14.2	X	X(ρ)	X,l	X	X							Tour X, Mt X	
V93-37	Ameroo (AM)	53.2	15.8	X	X(ρ)	X,l	X	X							Tour X, Mt X	
Average			13.0 ± 1.3													

[a] $\delta^{18}O$ in ‰SMOW

[b] Dist = distance measured northwards from Milandella (in km)

[c] Localities shown on Fig. 1

[d] Normal samples shown in plain text; Cordierite-Othoamphibole samples shown in *italics*; samples < 5 m from marbles in **bold**

hardest to constrain as these rocks lack geothermometry or barometry assemblages. Peak metamorphic temperatures in the lowermost biotite zone were probably ~ 350–400° C based on comparison with similar rocks in other terrains (e.g. Takasu 1987; Simon and Hoefs 1993). Pelites near Marne Reserve contain early kyanite that is replaced by andalusite and sillimanite (Sandiford et al. 1990) suggesting that pressures and temperatures in that part of the terrain were close to the aluminosilicate triple point (~ 580° C and 450–500 MPa). Temperatures for andalusite + staurolite rocks from the Lower Marne and Kappaluta localities were estimated by Dymoke and Sandiford (1992) using quantitative *P-T* pseudosections in the K_2O-FeO-MgO-Al_2O_3-SiO_2-H_2O system as ~ 565° C and ~ 580° C, respectively at 400–500 MPa. Temperatures for garnet + biotite-bearing samples at a number of localities in the high-grade part of the terrain were calculated using the garnet-biotite geothermometer of Ferry and Spear (1978). Pressues

Table 2 Mineralogy and stable isotope geochemistry of marbles from the Mount Lofty Ranges Abbreviations: *Amp* tremolitic amphibole, *Ap* apatite, *Cc* calcite, *Chl* chlorite, *Cz* clinozoisite, *Di* diopside, *Ep* epidote, *Gr* grossular, *Ksp* K-feldspar, *Musc* muscovite, *Mt* magnetite, *Plg* plagioclase, *Phl* phlogopite, *Py* pyrite, *Qtz* quartz, *Scp* scapolite, *Sph* sphene, *Ta* talc, *Tur* tourmaline, *Woll* wollastonite, *X* peak metamorphic mineral, *L* late Mineral

Sample	Location[a]	Dist[b]	$\delta^{18}O^{c}$	$\delta^{13}C^{c}$	Wt%Cc	Qtz	Di	AmpTa	Phl	Scp	Ksp	Plg	Other	Shear[e]
V92-34	Milendella (MD)	0.0	*13.0*[d]	*−0.9*[d]	29	X	X			X	X	X	Mt(X), Sph(X)	US
V92-35	Milendella (MD)	0.0	*13.1*	*−0.7*	33	X	X			X	X	X	Tur(X)	US
V92-36	Milendella (MD)	0.0	*12.8*	*0.2*	55	X	X			X	X	X	Tur(X), Woll (X)	US
V93-16	Milendella (MD)	0.0	*11.9*	*−1.3*	21	X	X				X	X	Woll(X), Gr(X)	US
V93-17	Milendella (MD)	0.0	*12.1*	*−1.3*	25	X	X				X	X	Woll(X), Gr(X)	US
V92-108	Emu Creek (EC)	3.1	13.9	0.0	73	X	X	X				X	Tur(X),Zir(X)	S
V92-109	Emu Creek (EC)	3.1	14.5	0.7	77	X	X	L		X			Mt(X)	MS
V92-110	Emu Creek (EC)	3.1	17.3	0.2	72	X	X			X		X	Ep(L)	S
V92-111	Emu Creek (EC)	3.1	15.2	−0.2	67	X	X			X	X			S
V92-114	Emu Creek (EC)	3.1	13.2	−1.5	65	X	X			X			Mt(X)	MS
V92-123	Cooke Hill (CH)	6.8	14.7	2.1	71	X	X		X		X			S
V92-124	Cooke Hill (CH)	6.8	14.8	1.8	73	X	X		X		X			S
V92-125	Cooke Hill (CH)	6.8	16.1	2.7	68	X	X		X	X	X			S
V92-126	Cooke Hill (CH)	6.8	15.3	1.1	70	X	X		L		X			S
V92-127	Cooke Hill (CH)	6.8	17.1	1.4	72	X	X				X		Sph(X),Chl(X)	MS
V92-128	Cooke Hill (CH)	6.8	13.8	−1.1	69	X	X		L		X		Mt(X)	S
V92-14	Lower Saunders Creek (LSC) Mbl1[f]	8.0	18.1	1.9	60	X	X	X	L	X		L	Cz (L)	US
V92-15	Lower Saunders Creek (LSC) Mbl1	8.0	17.0	1.4	62	X	X	X	L	X		L	Cz (L)	US
V92-16	Lower Saunders Creek (LSC) Mbl1	8.0	17.1	1.6	66	X	X	L		X		L	Cz (L), Mt (X)	MS
V92-17	Lower Saunders Creek (LSC) Mbl2	8.0	19.6	2.5	80	X	X		L	X				S
V92-18	Lower Saunders Creek (LSC) Mbl2	8.0	19.2	2.9	78	X	X		L	X				MS
V92-19	Lower Saunders Creek (LSC) Mbl2	8.0	19.7	2.9	66	X	X		X	X			Tur(X), Chl(L)	MS
91-AF-18	Upper Saunders Creek (USC)	8.6	**11.9**	**2.2**	68	X	X		X			X		US
91-AF-19	Upper Saunders Creek (USC)	8.6	**11.5**	**2.1**	68	X	X		X			X		US
91-AF-20	Upper Saunders Creek (USC)	8.6	**12.2**	**2.1**	62	X	X		X			X		US
91-AF-21	Upper Saunders Creek (USC)	8.6	**14.8**	**2.2**	65	X	X		X	X			Ap(X)	US
91-AF-22	Upper Saunders Creek (USC)	8.6	**14.4**	**2.4**	63	X	X		X	X		L		US
91-AF-23	Upper Saunders Creek (USC)	8.6	16.2	2.4	64	X	X		X	X		L		US
91-AF-24	Upper Saunders Creek (USC)	8.6	15.9	2.6	71	X	X		X	X				US
91-AF-27	Upper Saunders Creek (USC)	8.6	**10.8**	**2.6**	69	X			X				Mt(X)	US
91-AF-30	Upper Saunders Creek (USC)	8.6	**14.3**	**2.7**	72	X			X				Mt(X)	US
V93-59	Rishmin Valley (RV)	11.7	18.3	3.1	80	X	X		X	X				MS
V93-60	Rishmin Valley (RV)	11.7	20.1	3.6	82	X	X		X	X				US
91-AF-37	Trough Gully (TG) Mbl2[f]	13.0	**13.2**	**1.3**	74	X	X		X	X			Spn (X)	US
91-AF-38	Trough Gully (TG) Mbl2	13.0	**12.7**	**0.2**	71	X	X		X	X				MS
V92-60	Trough Gully (TG) Mbl2	13.0	20.7	3.9	72	X			X	X			Mt(X)	MS
V92-64	Trough Gully (TG) Mbl2	13.0	20.0	3.5	87	X			X	X			Mt(X)	MS
V92-67	Trough Gully (TG) Mbl2	13.0	20.4	3.2	86	X	X		X	X			Mt(X)	S
V92-81	Trough Gully (TG) Mbl1	13.0	15.3	2.4	75	X	X		X	X			Ap(X)	MS
V92-82	Trough Gully (TG) Mbl1	13.0	16.6	2.8	65	X	X		X	X				MS
V92-83	Trough Gully (TG) Mbl1	13.0	**14.9**	**1.4**	31	X	X		X	X				MS
V92-193	Marne Reserve (MR)	14.3	19.4	3.4	72	X			X	X				MS
V92-194	Marne Reserve (MR)	14.3	20.4	3.9	74	X	X		X	X			Mt (X)	MS
V92-204	Marne Reserve (MR)	14.3	**15.7**	**1.9**	77	X			X				Chl (L), Musc (L)	MS
V92-205	Marne Reserve (MR)	14.3	**17.5**	**2.9**	62	X	X		X	X	X			MS
V92-207	Marne Reserve (MR)	14.3	**18.2**	**2.6**	66	X	X						Ap(X)	US
V93-10	Nunkuri (NK)	18.8	19.0	3.0	68	X	X	X	X			X		MS
V93-12	Nunkuri (NK)	18.8	18.7	2.9	66	X		X	X			X		MS
V93-53	Kappalunta (KP)	19.1	19.8	3.6	67	X		X						US
V92-152	Kappalunta (KP)	19.1	17.2	3.6	69	X								US
91-AF-56	Pine Hut Road 1 (PH1)	22.3	17.6	3.1	70	X		X						US
V92-52	Pine Hut Road 1 (PH1)	22.3	18.0	3.0	69	X							Musc (X)	US
V93-7	Pine Hut Road 1 (PH1)	22.3	18.2	3.5	58	X						X	Musc (X)	US
V93-8	Pine Hut Road 1 (PH1)	22.3	19.6	3.4	50	X		X					Musc (X)	US
V93-9	Pine Hut Road 1 (PH1)	22.3	20.1	3.3	60	X						X	Musc (X)	US
V93-45	Keyneton (KY)	28.5	21.3	3.2	79	X			X					US
V93-46	Keyneton (KY)	28.5	20.9	3.0	87	X			X					US

Table 2 (continued)

Sample	Location[a]	Dist[b]	$\delta^{18}O^c$	$\delta^{13}C^c$	Wt%Cc	Qtz	Di	AmpTa	Phl	Scp	Ksp	Plg	Other	Shear[e]
V93-1	Sedan Road (SR)	29.1	22.8	3.0	76	X			X			X	Ap(X)	US
V93-2	Sedan Road (SR)	29.1	22.3	3.0	70	X								US
V93-3	Sedan Road (SR)	29.1	22.4	3.2	75	X			X					US
V93-4	Sedan Road (SR)	29.1	21.0	3.3	62	X			X					US
V93-40	Pipeline (PL)	35.5	19.0	3.2	87	X						X	Mt(X)	US
V93-41	Pipeline (PL)	35.5	19.5	3.3	85	X			X				Mt(X)	US
V93-27	Baldon South (BS)	39.8	22.0	3.4	81	X						X		US
V93-28	Baldon South (BS)	39.8	22.6	3.6	82	X						X		US
V93-23	Baldon North (BN)	41.3	20.3	3.3	73	X		X					Ap (X)	US
V93-24	Baldon North (BN)	41.3	20.2	3.2	75	X								US
V92-41	North Sturt Highway (NSH)	46.0	22.9	3.4	88	X		X				X		US
V92-42	North Sturt Highway (NSH)	46.0	21.8	3.7	80	X		X			X	X	Py(X), Mt(X)	US
V93-20	North Sturt Highway (NSH)	46.0	23.1	3.9	87	X		X				X		US
V93-21	North Sturt Highway (NSH)	46.0	23.4	3.2	82	X		X			X	X	Mt(X)	US

[a] Localities shown on Fig. 1
[b] Dist = distance measured northwards from Milandella
[c] $\delta^{18}O$ and $\delta^{13}C$ of calcite (‰ SMOW), ‰ PDB
[d] Normal samples shown in plain text; Milandella sharns shown in *italics*; samples = 5 m from pelites shown in **bold**
[e] *S* sheared, *MS* moderately sheared, *US* unsheared
[f] Mbl1 and Mbl 2 = adjacent marble layers

Table 3 Sumary of *P-T* estimates for the Mount Lofty Ranges

Location (Fig. 1)	*T*(°C)	*P*(MPa)	Notes
Milandella (MD)	700		a
Saunders Camp (SC)	680	430	b
Trough Gully (TG)	600		c
Marne Reserve (MR)	580	400–500	d
Upper Marne (UM)	565		e
Ruin (RU)	520		b
Kappalunta (KP)	560		e
Sturt Highway (SH)	350		f

[a] Estimated temperature of melting (see text)
[b] Garnet-biotite (Ferry and Spear 1978) and garnet-aluminosilicate-plagioclase-quartz (Newton and Haselton 1981) – Cartwright, unpublished data
[c] Garnet-biotite (Ferry and Spear 1978) – Arnold and Sandiford (1990)
[d] Aluminosilicate triplepoint (Sandiford et al. 1990)
[e] Quantitative pseudosections (Dymoke and Sandiford 1992)
[f] Estimated temperature of lowermost biotite zone (see text)

in garnet + sillimanite + quartz + plagioclase-bearing pelites at Saunders Camp were estimated at 430 MPa using the GASP geobarometer of Newton and Haselton (1981). The formation of migmatites in the higher-grade portions of the terrain suggests that temperatures were above the minimum melting curves, such as muscovite + K-feldspar + quartz + H_2O = melt that at 400–500 MPa lies at ~ 700° C at $XH_2O = 1$ (Thompson 1982). Overall, the mineral assemblages in the Mount Lofty rocks indicate that peak-metamorphic temperatures varied systematically from ~ 350–400 to ≥ 700° C over 50–55 km, corresponding to an average metamorphic field gradient of ~ 6–7° C/km (Table 3).

Figure 2 is a T-XCO_2 section in the system K_2O-CaO-MgO-Al_2O_3-SiO_2-H_2O-CO_2 (KCMAS) at 400 MPa constructed using the GE0-CALC computer programme of Berman et al. (1987) and the thermodynamic data of Berman (1988) that shows selected reactions between anorthite, calcite, diopside, dolomite, grossular, K-feldspar, muscovite, phlogopite, talc, tremolite, quartz, wollastonite, and a CO_2-H_2O fluid. Minerals in the Mount Lofty marbles contain some non-KCMAS components (notably Fe) that increase the variance of the mineral assemblages; however, since the minerals in the Mount Lofty marbles have compositions close to those in the KCMAS system (I. Cartwright, unpublished data), and as the general form of T-XCO_2 diagrams is not changed by minor amounts of additional components, Fig. 2 may be used to illustrate the progressive changes in marble mineralogy.

The lowest-grade marbles (at North Sturt Highway and Baldon North) contain quartz + calcite + talc assemblages that lie between reactions (2) and (3). Rocks at Pipeline, Sedan Road, and Kyneton contain calcite + phlogopite + quartz that constrains XCO_2 values to be between reactions (5) and (2). Marbles at Pine Hut Road 1 contain calcite + muscovite + quartz ± tremolite assemblages that lie below reaction (11) and above reaction (4). Marbles at Kappaluta that contain calcite + quartz + tremolite lie between reactions (4) and (6), while calcite + quartz + tremolite + phlogopite ± diopside assemblages at Nunkuri lie between reactions (4) and (2). The highest-grade marbles (at Lower Saunders Creek, Upper Saunders Creek, Cooke Hill, Emu Creek, and Milendella) contain calcite + quartz + diopside assemblages that lie

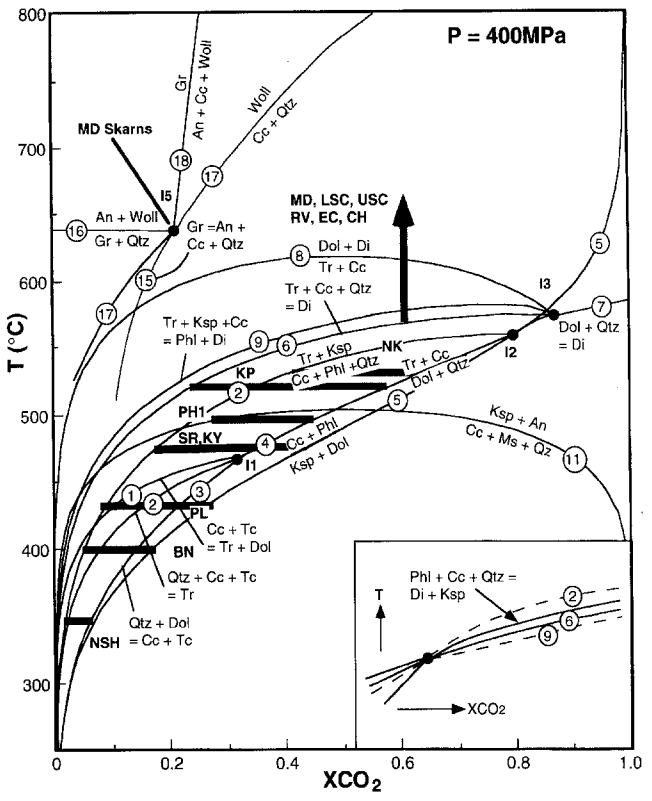

Fig. 2 T-XCO_2 section in the system K_2O-CaO-MgO-Al_2O_3-SiO_2-H_2O-CO_2(KCMAS) at 400 MPa constructed using the GEO-CALC computer program (Berman et al. 1987) and the internally consistent dataset of Berman (1988) showing selected reactions between anorthite, calcite, diopside, dolomite, grossular, K-feldspar, muscovite, phlogopite, talc, tremolite, quartz, and wollastonite (abbreviations as for Table 2). The *shaded lines* indicate the approximate XCO_2 values and temperatures recorded by the Mount Lofty marbles (data from Table 2 and Fig. 1)

above reaction (6) and at higher XCO_2 values than reaction (17). The phlogopite + diopside + calcite + quartz assemblage from Lower and Upper Saunders Creek is not predicted to be stable because phlogopite + calcite + quartz should react to form tremolite + K-feldspar at reaction (2) at lower temperatures than reaction (6). Phlogopite may have persisted metastabily in these rocks; alternatively, slight changes to the geometry of reactions in Fig. 2 are possible due to the relative partitioning of minor components (especially F and Fe) between phlogopite, diopside, and tremolite (e.g. Valley et al. 1990; Cartwright and Valley 1991). In this alternate topology (inset in Fig. 2), reaction (10): phlogopite + calcite + quartz = diopside + K-feldspar is stable and reactions (2) and (9) are metastable. The marbles adjacent to the granite at Milendella contain the assemblage calcite + quartz + wollastonite + grossular + diopside + plagioclase that is stable at the isobarically invariant point I5. While additional components will increase the variance of this assemblage, these rocks still lie on reaction (17), the position of which is largely unaffected by non-KCMAS components. While Fig. 2 is obviously simplified in as much as it is an end-member system, it is evident that, aside from the Milendella rocks, the marbles define a general increase in XCO_2 with increasing grade suggesting that prograde metamorphism took place largely under conditions of internal buffering. The trend of XCO_2 increasing with increasing temperature is also similar to that predicted to result from the up-temperature flow of water-rich fluids where time-integrated fluid fluxes are not excessive (e.g. Ferry 1994).

Stable isotope data

Whole rock $\delta^{18}O$ values of the metapelites and the granites are summarised in Table 1 and Fig. 3, and $\delta^{18}O$ and $\delta^{13}C$ values from calcite in the marbles are summarised in Table 2 and Fig. 4. Little mineral separation was attempted due to the fine grain size of the metasediments (especially at low grade) and the preponderance of porphyroblasts that contain abundant (up to 50 vol. %) inclusions.

Granites

The Palmer granite and the Rathjen gneiss, which were emplaced during regional metamorphism (Foden et al. 1990), have $\delta^{18}O$ values of 8.4–8.6‰ that are typical of granites (Taylor and Sheppard 1986). The quartz-biotite fractionations from these granites are 4.5–5.2‰, which are close to those reported by Bottinga and Javoy (1975) for granitic rocks (4.9 ± 1.4‰). Hence, these granites appear to preserve little-reset igneous oxygen isotope ratios.

Metapelites

The metapelites have been subdivided into three categories: (1) "normal" metapelites that represent the bulk of the rocks; (2) metapelites from within 5 m of marble layers that are used to constrain across-strike fluid flow; (3) orthoamphibole-bearing metapelites. The normal metapelites have $\delta^{18}O$ values that range from 15.8 to as low as 9.0‰ (Table 1, Fig. 3a,b). The higher of these values are within the "typical" range for pelitic metasediments (e.g. Hoefs 1980; Taylor and Sheppard 1986). The $\delta^{18}O$ values decrease with increasing metamorphic grade; normal metapelites from the biotite, andalusite-staurolite, sillimanite, and migmatite zones have average $\delta^{18}O$ values of 13.0 ± 1.3‰, 11.8 ± 0.9‰, 11.1 ± 0.9‰, and 10.5 ± 0.9‰, respectively (Fig. 3b). However, the decrease in $\delta^{18}O$ values is irregular and

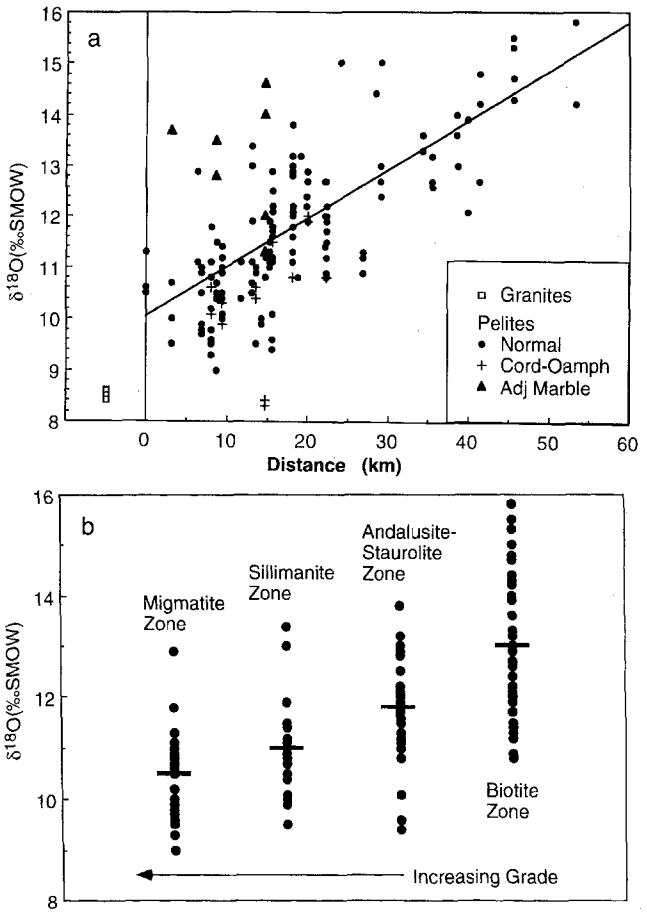

Fig. 3a, b Stable isotope geochemistry of the Mount Lofty Ranges metapelites and granites (data from Table 1). **a** $\delta^{18}O$(WR) values versus distance measured northwards from Milendella (Fig. 1). There is a general decrease in $\delta^{18}O$ of the normal metapelites with metamorphic grade (line is a best fit to these data). The metapelites collected within 5 m of the marbles (*Adj-Marble*) have higher $\delta^{18}O$ values than the normal metapelites, while the cordierite + orthoamphibole rocks (*Cord-Oamph*) have relatively low $\delta^{18}O$ values. **b** Summary of range and average $\delta^{18}O$ values of metapelites from the biotite, andalusite-staurolite, sillimanite, and migmatite zones

there is a spread of $\delta^{18}O$ values of several permil at any given grade. Figure 5 shows groups of samples collected from areas of $\sim 5\,m \times 5\,m$ separated by tens to hundreds of metres at the Lower Saunders Creek, Trough Gully, and Lower Marne localities. These data suggest that the metapelites may show large scale variations in $\delta^{18}O$ values, while being more isotopically homogeneous at metre scales. Metapelites from within 5 m of marble layers generally have higher $\delta^{18}O$ values than normal metapelites at the same grade, and $\delta^{18}O$ values decline with distance from the marble-metapelite contact (Fig. 6). The orthoamphibole-bearing metapelites lie within the general trend of the data, but have lower $\delta^{18}O$ values (down to 8.3‰) than the normal metapelites at the same metamorphic grades.

Marbles

The marbles are subdivided into: (1) "normal" marbles that represent the bulk of the rocks; (2) marbles from within 5 m of the contact with pelites that are again used to constrain across-strike fluid flow; (3) the garnet + wollastonite-bearing skarned marbles from Milendella. The normal marbles have $\delta^{18}O$(Cc) values that vary from 23.4‰ to as low as 13.2‰ (Table 2) which, as for the metapelites, range from little-altered to those typically found in areas affected by metamorphic fluid flow (e.g. Valley 1986). There is again a general but heterogeneous decrease in $\delta^{18}O$ values with increasing metamorphic grade. At two localities (Lower Saunders Creek and Trough Gully) there is a distinct difference in $\delta^{18}O$(Cc) values between adjacent marble layers that are separated by around 50 to 100 m. (Fig. 4a), again indicating that $\delta^{18}O$ values may vary by several permil over large scales whilst being more homogeneous at smaller scales. Within the normal marbles $\delta^{13}C$ values range from 3.8 to −1.6‰ (with most in the range 3.8 to 1.0‰), and there are broad correlations between $\delta^{18}O$(Cc) and $\delta^{13}C$(Cc) and $\delta^{13}C$ and metamorphic grade (Fig. 4b, c). Marble from within 5 m of the metapelites have lower $\delta^{18}O$ values than the normal marbles, and there is a general increase in $\delta^{18}O$ with distance from the metapelite layers (Fig. 6). Marbles adjacent to the pelites also tend to have slightly lower $\delta^{13}C$ values than the normal marbles at the same localities (Fig. 4c). The skarned marbles at Milendella have the lowest $\delta^{18}O$ values (11.9–13.1‰) and low $\delta^{13}C$ values (0.2–1.3‰); as discussed below, these marbles were probably infiltrated by fluids emanating from the adjacent granite. The normal marbles and those adjacent to the pelites contain 60–85wt% calcite, and with the exception of a few samples, there is a small but regular decrease in wt% calcite with increasing metamorphic grade (Fig. 4d). The skarned marbles have lower calcite contents (20–55 wt%).

Discussion

Stable isotope ratios may change in response to processes that occur at any time during the geological history of a terrain. As far as can be ascertained, the original nature of the sediments in the Mount Lofty Ranges does not appear to change markedly with grade. In particular, the marbles do not show any appreciable difference in carbonate content that could produce lower $\delta^{18}O$ values due to mixing of clastic and carbonate components. Additionally, there is no reason why sedimentary changes in both the metapelites and marbles would produce similar $\delta^{18}O$ vs distance trends. Hence, we conclude that the trends in stable isotope values identified above reflect metamorphic processes. The changes in oxygen isotope ratios in both the marbles and metapelites are too large to be simply

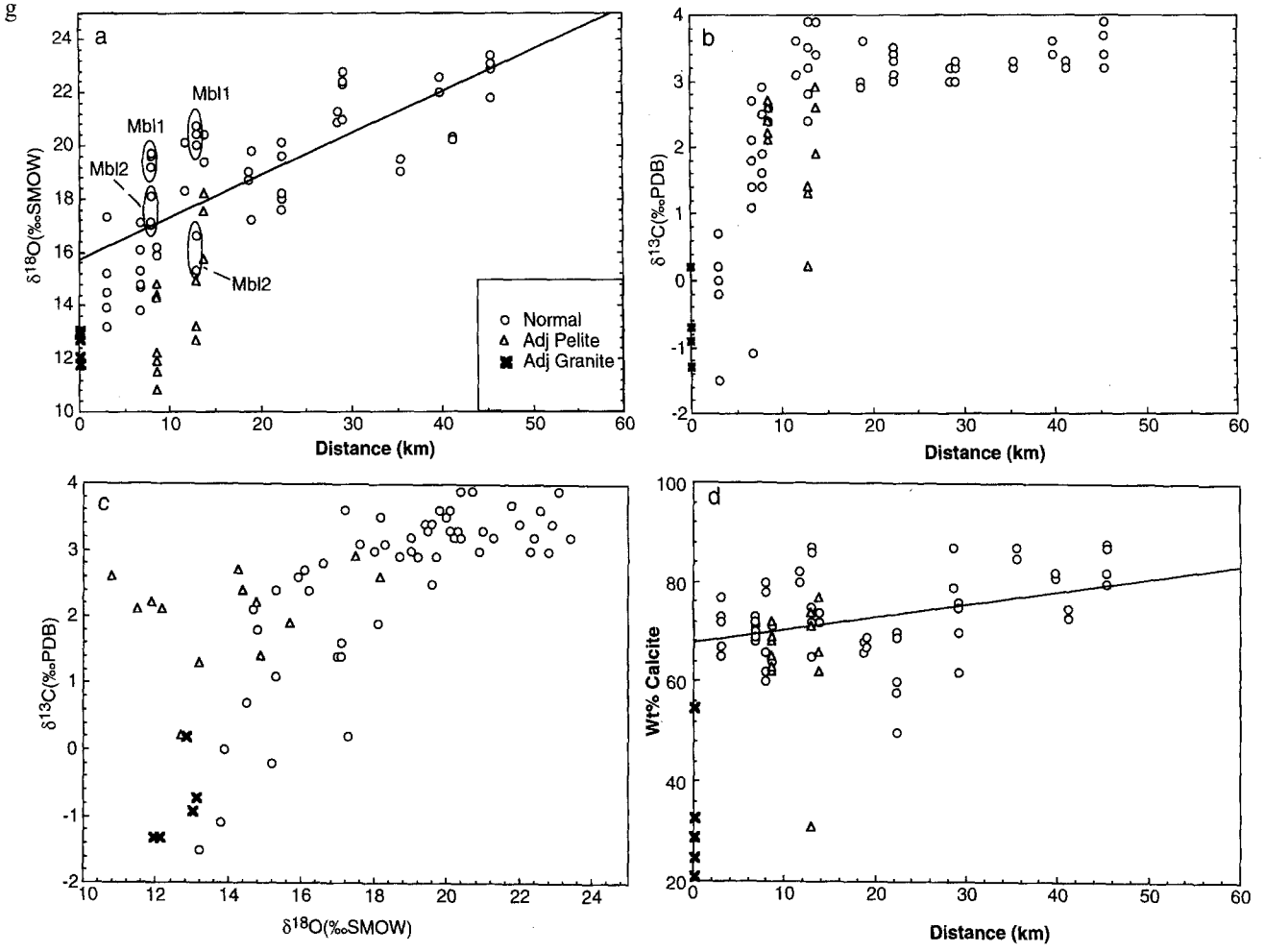

Fig. 4a–d Stable isotope geochemistry of Mount Lofty Ranges marbles (data from Table 2). **a** $\delta^{18}O(Cc)$ versus distance measured northwards from Milendella (Fig. 1). The normal marbles show an heterogeneous decrease in $\delta^{18}O(Cc)$ values with metamorphic grade. *Mbl 1* and *Mbl 2* are adjacent marble layers from single localities. Samples collected within 5 m of the metapelites (*Adj Pelite*) and skarned samples from Milendella have relatively low $\delta^{18}O(Cc)$ values. **b** $\delta^{13}C(Cc)$ versus distance. $\delta^{13}C$ values generally decrease towards high metamorphic grades. The skarned marbles and those adjacent to the pelites tend to have slightly lower $\delta^{13}C$ values than normal marbles at the same grades. **c** $\delta^{18}O(Cc)$ versus $\delta^{13}C(Cc)$. The normal marbles and those adjacent to the granite define an L-shaped $\delta^{18}O$-$\delta^{13}C$ trend that is broadly consistent with the infiltration of water-rich fluids. **d** Wt% calcite in the marble versus distance

the result of devolatilisation, suggesting that these changes were most probably caused by fluid infiltration. While some of the metapelites show minor retrogression, there is no correlation of $\delta^{18}O$ values with the degree of retrogression (Table 1), suggesting that the overall pattern of isotopic resetting is not a function of late, low-temperature fluid flow (although minor isotopic resetting may have occurred during retrogression). Also, given the lack of evidence for contact metamorphism, we conclude that fluid flow occurred during the regional metamorphism.

Fluid flow models

The following models of fluid flow will be considered: down-temperature fluid flow; across-strike fluid flow; and up-temperature fluid flow.

Down-temperature fluid flow

The oxygen isotope values of the metapelites and marbles at high metamorphic grades approach those of the granitic plutons (Tables 1, 2; Figs. 3, 4). Down-temperature fluid flow from the granites into the surrounding metasediments would have involved flow of an exotic fluid into the country rocks. Fluid flow under these circumstances produces a steep oxygen isotope front that migrates in the direction of the fluid (Nabelek 1991). Fluid-hosted diffusion will broaden any geochemical fronts; however, diffusive transport of oxygen isotopes during metamorphism probably only occurs over a few centimetres to a few metres (Bickle and Baker 1990a; Cartwright and Valley 1991; Cartwright 1994). Following down-temperature fluid flow, most

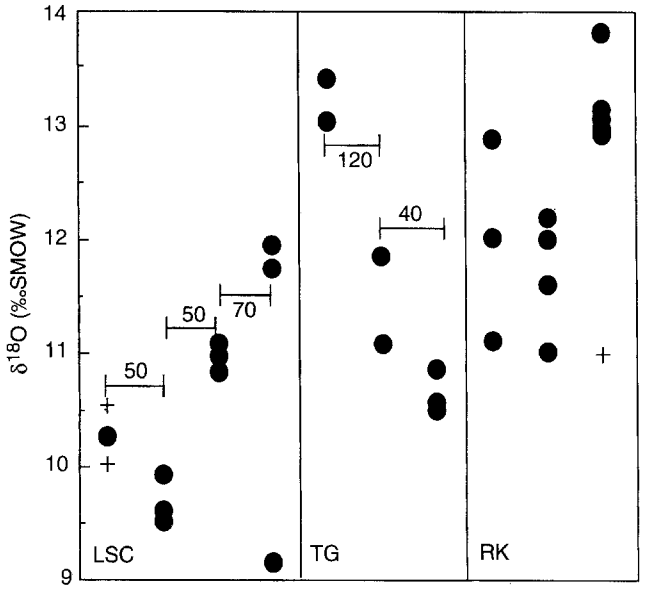

Fig. 5 Metre-scale variation in metapelites $\delta^{18}O$ values at the Lower Saunders Creek, Trough Gully, and Rocky Creak localities (data from Table 1). The metapelites show variation in $\delta^{18}O$ values of several ‰ over scales of a few tens of metres, whilst being more homogeneous on the metre scale, suggesting that across-strike fluid flow was limited. Symbols as for Fig. 3

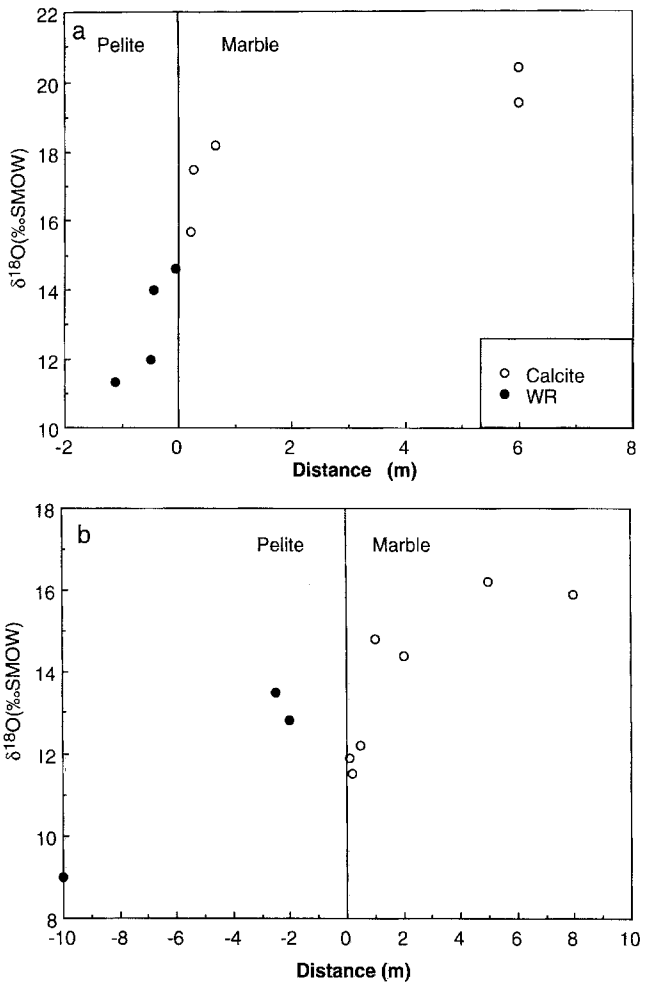

Fig. 6 $\delta^{18}O$ profiles across marble-metapelite boundaries at Upper Saunders Creek (**a**) and Marne Reserve (**b**) (data from Tables 1, 2). The steep $\delta^{18}O$ profiles which are bisected by the contacts together with the lack of low XCO_2 mineralogies in the marbles suggest that across-strike fluid advection was limited. Isotopic exchange at these contacts was probably by fluid-hosted diffusion

samples should lie either ahead of the isotopic front (unreset) or behind it (fully reset) with few samples lying on the front itself. In an ideal situation the preponderance of "partially reset" isotopic ratios, such as recorded in this study, would by itself indicate that down-temperature fluid flow was unlikely. However, regardless of the direction of fluid flow with respect to the temperature gradient, if fluid flow was channelled, transverse dispersion between high- and low-fluid flux zones could increase the volume of rock with partially reset isotopic ratios (e.g. Cartwright 1994). If fluid flow was rapid, incomplete isotopic exchange is possible and kinematic dispersion may become more prominent (Bowman et al. 1994). Both incomplete exchange and kinematic dispersion may produce broad isotopic fronts that increase the volume of rocks with partially reset isotopic ratios. Overall, the lack of distinct isotopic fronts is probably not a sufficient reason to rule out down-temperature fluid flow.

However, there are several problems with the down-temperature fluid-flow model. First, except for the skarned marbles directly adjacent to the granite at Milendella, the $\delta^{18}O$ values of the marbles and metapelites in the highest-grade rocks generally differ by several permil. Because mineral-mineral ^{18}O fractionations are small at high temperatures (Friedman and O'Neil 1977 and references therein), infiltration of a common fluid into the marbles and metapelites should result in these rocks having $\delta^{18}O$ values that are within 1–2‰ of each other. Additionally, again excluding the skarned marbles, the difference in $\delta^{18}O$ between the marbles and granites at high grades is 5–6‰. This is much larger than generally recorded in terrains where down-temperature fluid flow from igneous rocks into adjacent marbles has occurred (e.g. Nabelek 1991; Cartwright and Weaver 1993).

Second, the granites are a relatively small component of the terrain and are unlikely to have contained enough water to have caused the observed isotopic resetting. The time-integrated molar fluid flux (q_m) required to cause oxygen isotope resetting over a given distance (z, in m) is:

$$q_m = \frac{zV_{rk}}{N_{fl}} \qquad \text{(i)}$$

(Bickle and Baker 1990a; Dipple and Ferry 1992a; Bowman et al. 1994), where N_{fl} is the number of moles of O per mole of fluid ($N_{fl} = 1$ for H_2O), and V_{rk} is the number of moles of oxygen per m^3 of rock ($\sim 8.1 \times 10^4$, Robie et al. 1978). Resetting of oxygen isotopes over 55 km thus implies time-integrated fluid fluxes of

$\sim 4 \times 10^9$ moles/m^2. A crystallizing granite pluton ($\rho = 2500$ kg/m^3) that originally contains 10 wt% H_2O will liberate ~ 14000 moles of water per m^3 of granite. Hence, it requires a ~ 285 km thickness of granite to provide enough water to reset oxygen isotope ratios over 55 km. Even if extreme fluid channelling is invoked, it is difficult to envisage the relatively small volumes of granite in the Mount Lofty Ranges providing enough fluid to cause the observed isotopic resetting.

Third, the infiltration of water-rich fluids from the granite into the marbles would probably produce minerals such as wollastonite, vesuvianite, and grossular that are common in marbles that have been infiltrated by water-rich fluids during metamorphism (e.g. Valley et al. 1990; Tracy and Frost 1991; Cartwright and Weaver 1993; Cartwright and Oliver 1994). However, such minerals are extremely rare in the Mount Lofty Ranges where the majority of marbles have relatively high-$X\mathrm{CO}_2$ assemblages (Fig. 2). The volumes of fluid required to reset marble mineralogies are generally lower than those required to reset the oxygen isotope ratios; hence, marbles that have been infiltrated by water-rich fluids usually have reset mineralogies even where their stable isotope ratios are little reset (e.g. Bickle and Baker 1990b). Given that fluids emanating from granitic rocks are generally water rich (e.g. Cartwright and Weaver 1993; Bowman et al. 1994; Cartwright and Oliver 1994), the infiltration of sufficient fluid from the Mount Lofty Ranges granites to lower the oxygen isotope ratios over many kilometres should produce low-$X\mathrm{CO}_2$ assemblages in most of the marbles in the terrain.

Finally, fluid flow from granites often produces skarns where major element metasomatism has occurred (e.g. Nabelek 1991). However, there are no major skarns around any of the granites in the study area, and it seems unlikely that there was major lateral fluid flow out of the granites at the current level of exposure. Overall we consider it highly unlikely that large scale metamorphic fluid flow out of the granites has affected this terrain, although the marbles at Milendella that have low-$\delta^{18}O$ values and low-$X\mathrm{CO}_2$ assemblages most probably record local fluid flow from the adjacent granite.

Across-strike fluid flow

If fluid flow were more pervasive at higher metamorphic grades, across-strike flow could cause isotopic resetting of large regions of rock. However, this is unlikely to explain the pattern of isotopic resetting in the Mount Lofty Ranges because the steep gradients in $\delta^{18}O$ values of several permil over a few metres at the marble-metapelite contacts (Fig. 6) would not be preserved if significant across-strike fluid flow had occurred (e.g. Bickle and Baker 1990a; Cartwright and Valley 1991; Cartwright 1994). The mineralogy of the marbles also implies little fluid flow from the metapelites into the marbles. Because prograde metamorphism of pelites involves the breakdown of hydrous minerals, metamorphic fluids in the metapelites were probably water rich. The lack of minerals such as wollastonite, vesuvianite, grossular, and zoisite at most marble-metapelite contacts indicates that $X\mathrm{CO}_2$ values in the marbles were much higher than in the pelites (Fig. 2). Hence, the marble-metapelite contact represents a discontinuity in $X\mathrm{CO}_2$ values that also implies a lack of significant across-strike fluid flow.

Up-temperature fluid flow

As discussed above, it is unlikely that the Mount Lofty Ranges experienced significant down-temperature or across-strike fluid flow, suggesting that up-temperature fluid flow may be the most likely scenario. The patterns of oxygen isotope resetting in the metapelites and the marbles are similar to those predicted to occur during up-temperature fluid flow (Dipple and Ferry 1992a), and order-of-magnitude estimates of the fluid fluxes required to produce the observed resetting of oxygen isotopes may be made. In common with most studies of metamorphic flow (e.g. Bickle and McKenzie 1987; Bickle and Baker 1990a, Cartwright and Oliver 1995, Bowman et al. 1994), we make a number of assumptions and simplifications, these are: (1) fluid flow was unidirectional from low to high grade; (2) diffusion coefficients for oxygen are sufficiently low that diffusive transport only occurs over a few centimetres to metres; (3) the temperature profile did not vary through the infiltration event; (4) fluid-rock isotopic equilibration was rapid; (5) resetting of oxygen isotopes was solely by exchange with the fluid. These assumptions are assessed further below. The aim of these calculations is to provide order-of-magnitude estimates for the volumes of fluid and the boundary conditions of the flow system required to produce the observed resetting. With these simplifications, the resetting of $\delta^{18}O$ values at any point along the flow path is given by:

$$\delta^{18}O^f_{rk}(z) - \delta^{18}O^i_{rk}(z) = \delta^{18}O^i_{fl}\left(z - \frac{q_m N_{fl}}{V_{rk}}\right) - \delta^{18}O^i_{fl}(z) \qquad \text{(ii)}$$

(Dipple and Ferry 1992a) where the superscripts f and i refer to final and initial values, the subscripts fl and rk refer to the fluid and the rock, and other abbreviations are as for Eq. (i).

At any point along the flow path, the degree of isotopic resetting is proportional to the time-integrated fluid flux, the changes in the fluid-rock partition coefficient for ^{18}O with temperature, and the temperature gradient. Based on the metamorphic field gradient, temperature was assumed to vary linearly from 350° C

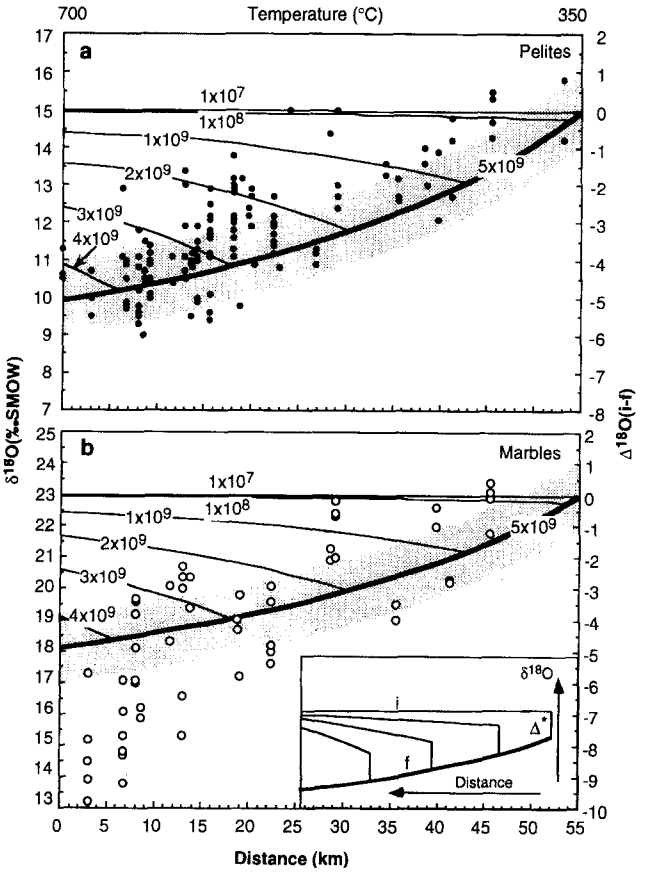

Fig. 7 Predicted resetting of $\delta^{18}O$ values of the metapelites (**a**) and marbles (**b**) due to up-temperature fluid flow calculated using Eq. (ii) and contoured for time-integrated fluid fluxes (in moles/m^2). The *lower curve* on the diagram represents $\delta^{18}O$ values that are in equilibrium with the fluid and the *shaded area* is $\pm 1‰$ of the equilibrium curve. The range in $\delta^{18}O$ values in both the marbles and the metapelites may be explained by time-integrated fluid fluxes varying by around an order of magnitude. If the fluid entering the marbles at low temperatures was not in isotopic equilibrium with these rocks, the discontinuities on the curves are transformed into discrete fronts where the front height (Δ^*) is the degree to which the fluid is out of isotopic equilibrium (*inset* in **b**). The maximum resetting possible in this case is a function of the temperature difference between the start and end of the flow path and Δ^*

to 700° C over 55 km ($dT/dz = 6.4°$ C/km). Isotopic resetting of the marbles was modelled using calcite-H_2O fractionation data, while that in the metapelites used the anorthite-H_2O fractionation data (Friedman and O'Neil 1977). These fractionations were chosen because they are close to the average rock-water fractionations for these rocks. Anorthite has equilibrium $\delta^{18}O$ values that are intermediate between felsic minerals, such as quartz, albite, and K-feldspar, and mafic minerals, such as micas, amphiboles, garnet, and oxides. Similarly calcite has equilibrium $\delta^{18}O$ values intermediate between quartz and minerals such as pyroxene, amphiboles, or micas (Friedman and O'Neil 1977). The fluid was assumed to be in isotopic equilibrium with the rocks at low grades and to maintain isotopic equilibrium at all points along the flow path.

Figure 7 shows the predicted pattern of resetting of $\delta^{18}O$ values of the marbles and metapelites due to up-temperature fluid flow, contoured for time-integrated fluid fluxes. The initial $\delta^{18}O$ value was taken as the average $\delta^{18}O$ value of the rocks at low grades (Figs. 3, 4). The lower curve on the diagram represents the $\delta^{18}O$ values that are in equilibrium with the fluid. In both cases resetting of oxygen isotope ratios along the entire flow path is achieved by time-integrated fluid fluxes of $\sim 5 \times 10^9$ moles/m^2 ($\sim 10^5$ m^3/m^2) or higher. For both sets of rocks, $\delta^{18}O$ values are predicted to be lowered by $\sim 5‰$. In the pelites, the maximum isotopic resetting at any temperature is close (to within 1‰) to the maximum resetting predicted by the model, and much of the variation in $\delta^{18}O$ values in the metapelites could be accounted for by time-integrated fluid fluxes varying by about one order of magnitude.

While the up-temperature model fits the observed isotopic resetting of the metapelites, the decrease in $\delta^{18}O$ values in the marbles at high grades is significantly greater (up to 8–9‰) than predicted by the model, which requires explanation. Most normal marbles at high grades contain $> 60\%$ calcite, suggesting that devolatilisation cannot account for the additional reduction in $\delta^{18}O$ values (e.g. Valley 1986). The model discussed above is relatively conservative in as much as it uses the lowest temperature measured in the area as the temperature at the fluid inlet and assumes that the fluids were in equilibrium with the pelites or the marbles at that temperatures. We chose to adopt this boundary condition as no lower-grade rocks are present in this part of the Adelaide Fold Belt (Offler and Fleming 1968). However, if temperatures at the inlet of the fluid-flow path were lower (for instance, if the fluid came from higher-level, cooler, rocks), the differences in fluid-rock ^{18}O fractionations between the rocks at the low- and high-temperature ends of the flow path would be greater, and the maximum amount of oxygen isotope resetting would consequently be larger. Alternatively, if the fluids entering the marble layer at low temperatures were partially derived from the pelitic rocks they would have lower $\delta^{18}O$ values than fluids in equilibrium with the marbles. This would transform the discontinuities in the isotopic profiles into definite fronts, and produce additional resetting of $\delta^{18}O$ values proportional to the degree that the mixed fluid was out of isotopic equilibrium. The marble mineral assemblages at low grades have low-XCO_2 values (Fig. 2), and the input of water-rich fluids from the pelites might not alter their mineralogy. Since the marbles are a minor component of the terrain, this explanation is possible. The marbles presently form a discontinuous layer, however there is no evidence for fluid flow from the pelites into the "ends" of the marble units. We consider that fluid flow either occurred prior to boudinage of the marble layer, or that the marbles are connected above or below the exposure surface.

The above model assumes a steady state temperature gradient that is unlikely to have been the case. The time-integrated fluid flux required to move the geochemical discontinuities or fronts a given distance is governed by the term N_{fl}/V_{rk} that is largely temperature independent. Additionally, if fluid-rock equilibrium is maintained, the $\delta^{18}O$ or $\delta^{13}C$ values may constantly adjust to a changing temperature gradient during fluid flow. Preliminary numerical modelling shows that this is possibly the case where the rate of change of the temperature gradient relative to the fluid fluxes is low (I. Cartwright, unpublished data). If the above assertions are correct, isotopic resetting will be a function of the time-integrated fluid-flux and the *final* temperature gradient during the fluid flow event. This is directly analogous to mineral assemblages continuously re-equilibrating during prograde metamorphism. Since there is little evidence for major retrogression of the Mount Lofty rocks, fluid flow probably did not continue for a significant time during cooling. We therefore consider that using the peak metamorphic field gradient as an approximation of the temperature gradient during fluid flow is justified.

Resetting of $\delta^{13}C$ values

If the fluids were carbon bearing, resetting of $\delta^{13}C$(Cc) values in the marbles should have occurred during up-temperature flow. Figure 8 shows the predicted $\delta^{13}C$(Cc) values for variable fluid fluxes along a temperature gradient of 6.4° C/km for fluids of $XCO_2 = 0.1$ to 0.5. The resetting of C isotopes was again calculated using Eq. (ii) for a rock with 65% calcite (V_{rk} for $C \approx 2 \times 10^4$ moles/m^3, Robie et al. 1978). Modelling the changes in C isotopes is complicated by changes in fluid composition along the flow path due to the progress of buffering reactions (Fig. 2); however, this can partly be overcome by considering a range of XCO_2 values. Calcite-fluid fractionation factors were calculated using the CO_2-calcite fractionation data of Chacko et al. (1991). An initial $\delta^{13}C$ value of 3.5‰ was assumed, similar to the average $\delta^{13}C$ value at low grades. The calculations predict that similar time-integrated fluid fluxes to those required to reset the oxygen isotopes should lower $\delta^{13}C$ values by up to 2‰ at high metamorphic grades; although the time-integrated fluid flux required to reset rocks at any given point on the flow path decreases as XCO_2 of the fluid increases. Except for a few high-grade samples, the degree of resetting of carbon isotopes in the normal marbles is within the range predicted by the model. Most of the resetting of $\delta^{13}C$(Cc) values occurs at relatively high grades (Fig. 4b). The up-temperature fluid flow model envisages that fluids were buffered to higher-XCO_2 values with increasing temperature along the flow path (Fig. 2). Hence, at low temperatures

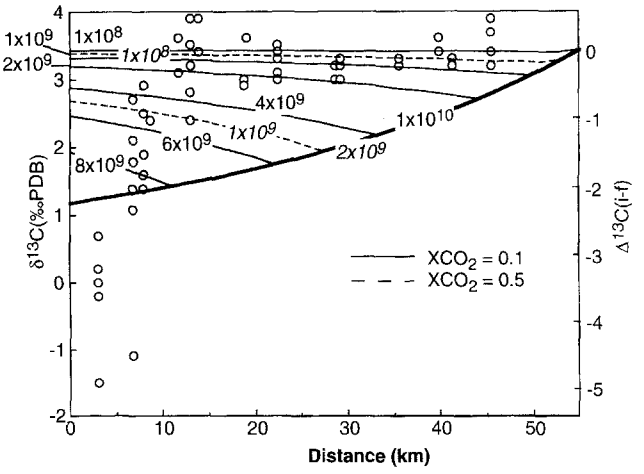

Fig. 8 Predicted resetting of $\delta^{13}C$(Cc) values during up-temperature fluid flow with fluids of $XCO_2 = 0.1$ and 0.5 and a rock with 65% calcite ($V_r = 2 \times 10^4$ moles/m^3, Robie et al. 1978). The $\delta^{13}C$ values should be lowered by up to 1.7‰ at high metamorphic grades by similar time-integrated fluid fluxes to those required to reset the oxygen isotope values

the carbon content of the fluid would have been low and even high-fluid fluxes would have produced little resetting of the $\delta^{13}C$ values. With increasing temperature, the increase in carbon content of the fluid would enhance its ability to reset the carbon isotopes. Figure 4c shows that $\delta^{18}O$(Cc) and $\delta^{13}C$(Cc) values in the marbles define an "L-shaped" trend that is similar to those predicted for the infiltration of water-rich fluids into marbles (Valley 1986). Overall, the resetting of the $\delta^{13}C$ values is broadly consistent with the up-temperature fluid-flow model.

Fluid fluxes and intrinsic permeabilities

If the duration of metamorphism is known, actual fluid fluxes may be calculated. From numerical modelling of the geometry of isotherms around folds, Sandiford et al. (1995) estimated that metamorphism in the Mount Lofty Ranges occurred over 1–3 Million years or less. Time scales of metamorphism of ~ 10 Ma have been estimated for other low-pressure high-temperature terrains (Christensen et al. 1989). Hanson (1992) estimated that fluid production and flow of internally derived fluids during regional metamorphism may last for up to 15 Ma. To encompass this range of estimates we will consider fluid flow lasting 0.1–10 Ma(3×10^{12}–3×10^{14} s). For this time period, a time-integrated fluid flux of 10^{10}–10^9 moles/m^2 yields an average actual fluid flux of 3×10^{-6}–3×10^{-3} moles/m^2/s. ($\sim 10^{-10}$–10^{-7} m^3/m^2/s). Intrinsic permeability is related to fluid flux via Darcy's Law:

$$v = \frac{-K_\phi}{\eta}\frac{dP}{dz} \qquad \text{(iii)}$$

(e.g. deMarsily 1986), where K_ϕ is the intrinsic permeability, η is the fluid viscosity ($\sim 10^{-4}$ Pa.s for H_2O at 500–600° C; Bickle and McKenzie 1987), v is the volumetric fluid flux, and dP/dz is the fluid-pressure gradient. Fluid-pressure gradients of –1500 Pa/m were suggested for contact metamorphic fluid flow around the Skaergaard intrusion by Norton and Taylor (1979), far below the gradient that results from buoyancy (approximately –19000 Pa/m). Using these fluid-pressure gradients, and fluid fluxes of 10^{-7} to 10^{-10} $m^3/m^2/s$ yields intrinsic permeabilities of 10^{-20} to 10^{-16} m^2. While these values are probably, at best, order-of-magnitude estimates, they do represent a test for the model. The estimated permeabilities are within the range of measured intrinsic permeabilities for metamorphic rocks (Brace 1980), and are similar to intrinsic permeabilities proposed for other metamorphic terrains (Bickle and Baker 1990a; Baumgartner and Ferry 1991; Léger and Ferry 1993; Cartwright 1994). They are also similar to the range of intrinsic permeabilities (10^{-19}–10^{-17} m^2) calculated by Hanson (1992) as necessary to permit large-scale fluid circulation in regional metamorphic terrains. These calculations suggest that the proposed fluid-flow regime in the Mount Lofty Ranges could have occurred over the likely duration of metamorphism with reasonable intrinsic permeabilities. As discussed above, the rocks probably record at least an order-of-magnitude variation in time-integrated fluid fluxes. If fluid flow occurred over the same time with the same fluid pressure gradient throughout the terrain, this would imply that intrinsic permeabilities also varied by around an order of magnitude. Similar local variations in intrinsic permeabilities have been proposed for other regional and contact metamorphic terrains (e.g. Ferry 1992; Cartwright and Weaver 1993; Cartwright and Buick 1994).

Other petrological and geochemical considerations

The mineralogical data from the marbles are broadly consistent with the up-temperature fluid-flow model. As long as fluid fluxes are not excessive and do not overcome the buffering capacity of the rocks, up-temperature fluid flow is predicted to produce a similar increase in XCO_2 values with increasing temperature to that seen in Fig. 2 (Baumgartner and Ferry 1991; Ferry 1994).

In the metapelites at Jo's Gully (Fig. 1), orthoamphibole + cordierite grew at the expense of biotite + staurolite at approximately peak metamorphic conditions. As there are no other K_2O-bearing minerals in these rocks, the breakdown of biotite probably involved K removal by fluids (Arnold and Sandiford 1990). One of the predicted consequences of up-temperature fluid flow is a reduction of K_2O in the rocks due to the changing solubility of K in the fluids (Dipple and Ferry 1992b). Hence, the orthoamphibole rocks may reflect zones of high-fluid fluxes where significant K depletion has occurred. The orthoamphibole rocks have relatively low $\delta^{18}O$ values (Fig. 3), suggesting that they may have experienced relatively high time-integrated fluid fluxes.

Metapelites at the highest grades in the Mount Lofty Ranges underwent partial melting during the regional metamorphism (Offler and Flemming 1968), and locally contain 40% leucosomes. Significant partial melting of pelitic rocks at $\sim 700°$ C probably requires the influx of externally derived fluids, especially as pelites at high grades contain biotite that defines peak metamorphic fabrics, suggesting that significant dehydration melting has not occurred. Fluids flowing up temperature may have fluxed melting at high metamorphic grades, and the formation of migmatites could have been a sink for fluids providing a barrier to further up-temperature fluid migration. During cooling, fluids would have been exsolved from the crystallising melts, and may have migrated upwards out of the terrain.

Overall pattern of fluid flow

The overall pattern for metamorphic fluid flow is shown in Fig. 9. We envisage up-temperature fluid flow towards the granite with minor fluid-flow out of the granites. Zones of major down-temperature fluid-flow with skarn formation are not recognised but may have existed above the granite plutons. Orthoamphibole rocks and migmatites were also formed as part of the fluid-flow system. It must be stressed that the up-temperature fluid flow model is favoured because most of the isotopic and mineralogical data may be explained by this model while the alternatives do not fit the available data. Given the potential complexities of large-scale metamorphic fluid flow, no single set of observations unambiguously indicates that up-temperature fluid flow occurred.

The up-temperature fluid-flow model requires a fluid source within the country rocks at low metamorphic grades. The devolatilisation of sediments at low grades may release large volumes of fluid. Clay minerals such as illite that are common in mudstones and shales contain ~ 9 wt% H_2O. Thus transformation of clays through chlorites to biotite (which contains ~ 4 wt% H_2O) will yield ~ 0.05 kg H_2O per kg of clay. If the metapelites initially contained 20–25% clay, the total yield of water would be ~ 0.01 kg per kg rock, which, assuming a density of 2700 kg/m^3, equates to 1500 $moles/m^3$. The total yield of water per m^3 of sediment may be less than that derived from granites; however, in the Mount Lofty Ranges, as in most metasediment-dominated metamorphic terrains, the largest total fluid source may be the sediments. If the fluid-flow system extended for long distances away from the

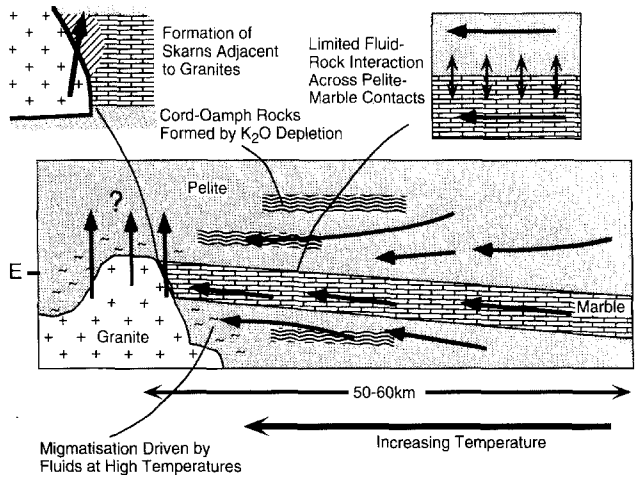

Fig. 9 Cartoon showing overall pattern of metamorphic fluid flow. Fluid flow was largely up-temperature towards the granite with minor fluid flow out of the granites. Zones of major down-temperature fluid flow with skarn formation are not recognised but may have existed above the granite plutons. Cordierite + orthoamphibole rocks were formed as part of the flow system due to K_2O being removed in the fluids and the influx of fluids caused partial melting at high metamorphic grades

metamorphic highs, circulating deep basinal fluids may also be a potential source. All that is required for the infiltration model is that the fluids were approximately in isotopic equilibrium with the pelitic rocks at the low-temperature end of the flow path.

The model requires that large-scale subhorizontal fluid flow occurred. Since fluid flow under lithostatic pressure is predicted to be vertical (due to buoyancy), the driving force for this flow requires explanation. For the proposed fluid flow to have occurred there was presumably a fluid-pressure gradient from low- to high-metamorphic grades (although there are no data with which to test this). In metasediments, the variation in intrinsic permeabilities between different layers will tend to channel fluids parallel to layering, and the presence of a few low permeability layers could inhibit across-strike, vertical, fluid flow. The dominant schistosity in the Mount Lofty Ranges (S2) is steeply dipping and strikes north–south. This fabric may have produced an anisotropy in hydraulic conductivity that may have also helped to channel fluid flow along the length of the terrain. It is also possible that the synmetamorphic D2 deformation caused sequential opening of microfractures that pumped fluid through the rocks. Up-temperature fluid flow will in general cause prograde devolatilisation reactions to progress (Baumgartner and Ferry 1991), and reaction-enhanced permeability may have promoted fluid flow. Layers of different compositions probably undergo metamorphic reactions (and hence permeability enhancement) at different times, which would also help promote layer-parallel fluid flow. As is common in studies of metamorphic fluid flow (e.g. as reviewed by Rumble 1994), the inferred volumes of fluid passing through the Mount Lofty rocks are large given our estimates of metamorphic porosities and permeabilities. While the up-temperature fluid-flow model presented above can explain the observed isotopic and petrological data, it is probably unrealistic to envisage a column of fluid passing uniformly through the rocks. The actual fluid-flow system may have been much more complicated, with fluid flow being alternately accommodated in fractures and along grain boundaries. Fluids may have also occasionally flowed across strike in channels not recognised in this study.

Comparisons with other terrains

A similar pattern of up-temperature metamorphic fluid flow with similar time-integrated fluid fluxes (10^8–10^9 moles/m^2) has been proposed for the Acadian terrain of Vermont, USA (Ferry 1992; Stern et al. 1992; Léger and Ferry 1993). The time-integrated fluid fluxes estimated by Ferry (1992) and Léger and Ferry (1993) are from calculations of reaction progress that are independent of the calculations of Stern et al. (1992) that were based on stable isotopes. That time-integrated fluid fluxes in separate terrains calculated by different methods are similar may reflect the processes of regional metamorphism in general. Both the Vermont and the Mount Lofty terrains are of similar size and record similar metamorphic conditions, and the time-integrated fluid fluxes may be related to the amount of fluid produced within a given crustal volume during metamorphism. By contrast, estimates of time-integrated fluid fluxes due to up-temperature fluid flow in contact aureoles are often an order of magnitude lower (e.g. 5×10^6–5×10^7 moles/m^2 in the Sierra Nevada, USA: Davis and Ferry 1993). The differences between the calculated time-integrated fluid fluxes in contact and regional metamorphic terrains may reflect differences in the total amount of fluid produced in a terrain due to the areal extent of metamorphism. Alternatively, since contact metamorphism is generally of shorter duration than regional metamorphism, the differences may relate to the volume of fluid that can physically pass through rocks over the duration of the metamorphic event.

While a number of regional metamorphic terrains do show decreasing $\delta^{18}O$ values with increasing metamorphic grade many do not, indicating that the type of fluid-flow regime proposed here is not ubiquitous. For instance the Reynolds Range, central Australia, is a similar size terrain to the Mount Lofty Ranges that preserves a regional metamorphic temperature gradient from greenschist to granulite facies (e.g. Buick et al. 1994). The Reynolds Range also contains abundant metasediments, but metapelites and marbles in this terrain show no correlation of $\delta^{18}O$ values with metamorphic grade (I.S. Buick and I. Cartwright

unpublished data). However, the Reynolds Range underwent widespread fluid-rock interaction during contact metamorphism prior to the regional metamorphism (Buick et al. 1994) that may have sufficiently dehydrated the rocks, resulting in little fluid being present during the regional event. We suggest that fluid-flow regimes of the type proposed for the Mount Lofty Ranges are most likely to affect metasediment-dominated terrains that lack an earlier contact metamorphic history.

Acknowledgments We thank J. Lee, S. Zakowski and R. Smakman for help with sample preparation and isotope analyses. D. Gelt drafted Figs. 1 and 9. S. Golding and T. Weaver provided helpful comments. This work was supported by ARC grant A39231141 and a QEII fellowship (to I.C.) and an ARC Postdoctoral fellowship (to J.K.V.).

References

Arnold J, Sandiford M (1990) Petrogenesis of cordierite-orthoamphibole assemblages from the Springton region, South Australia. Contrib Mineral Petrol 106:100–109

Baumgartner LP, Ferry JM (1991) A model for coupled fluid-flow and mixed-volatile mineral reactions with applications to regional metamorphism. Contrib Mineral Petrol 106:273–285

Berman RG (1988) Internally consistent thermodynamic data for stoichiometric minerals in the system Na_2O-K_2O-CaO-MgO-FeO-Fe_2O_3-Al_2O_3-SiO_2-TiO_2-H_2O-CO_2. J Petrol 29:445–522

Berman RG, Brown TH, Perkins EH (1987) GE0-CALC: software for calculation and display of *P-T-X* phase diagrams. Am Mineral 72:861–862

Bickle MJ, Baker J (1990a) Advective-diffusive transport of isotopic fronts: an example from Naxos, Greece. Earth Planet Sci Lett 97:78–93

Bickle MJ, Baker J (1990b) Migration of reaction and isotopic fronts in infiltration zones: assessments of fluid flux in metamorphic terrains. Earth Planet Sci Lett 98:1–13

Bickle MJ, McKenzie DM (1987) The transport of heat and matter by fluids during metamorphism. Contrib Mineral Petrol 95:384–392

Bottinga Y, Javoy M (1975) Oxygen isotope partitioning among minerals in igneous and metamorphic rocks. Rev Geophys Space Phys 13:401–418

Bowman JR, Willett SD, Cook SJ (1994) One-dimensional models of oxygen isotopic transport and exchange during fluid flow: constraints from spatial patterns of oxygen isotopic compositions on fluid fluxes and flow parameters. Am J Sci 294:1–55

Brace WF (1980) Permeability of crystalline and argillaceous rocks. Int J Rock Mech Min Sci 17:241–251

Buick IS, Cartwright I, Hand M, Powell R (1994) Evidence for pre-regional metamorphic fluid infiltration of the Lower Calcsilicate Unit, Reynolds Range Group (central Australia). J Metamorphic Geol 12:789–810

Cartwright I (1994) The two-dimensional pattern of metamorphic fluid flow at Mary Kathleen, Australia: fluid focussing, transverse dispersion, and implications for modelling fluid flow. Am Mineral 79:526–535

Cartwright I, Buick IS (1994) Channelled fluid infiltration in calcsilicates and variations in fluid fluxes and intrinsic permeabilities. J Geol Soc, London 151:583–586

Cartwright I, Oliver NHS (1994) Fluid flow during contact metamorphism: Mary Kathleen, Queensland, Australia. J Petrol 35:1493–1519

Cartwright I, Valley JW (1991) Steep oxygen-isotope gradients at marble-metagranite contacts in the northwest Adirondack Mountains, New York, USA: products of fluid-hosted diffusion. Earth Planet Sci Lett 107:148–163

Cartwright I, Valley JW (1992) Oxygen-isotope geochemistry of the Scourian complex, NW Scotland. J Geol Soc London 149:115–126

Cartwright I, Weaver TR (1993) Metamorphic fluid flow at Stephen Cross Quarry, Québec: stable isotopic and petrological data. Contrib Mineral Petrol 113:533–544

Chacko T, Mayeda TK, Clayton RN, Goldsmith JR (1991) Oxygen and carbon fractionations between CO_2 and calcite. Geochim Cosmochim Acta 55:2867–2882

Chamberlain CP, Ferry JM, Rumble D III (1990) The effect of net-transfer reactions on the isotopic composition of minerals. Contrib Mineral Petrol 105:322–336

Christensen JN, Rosenfeld JL, DePaulo DJ (1989) Rates of tectonometamorphic processes from rubidium and strontium isotopes in garnet. Science 244:1465–1469

Clayton RN, Mayeda TK (1963) The use of bromine pentafluoride in the extraction of oxygen from oxides and silicates for isotopic analysis. Geochim Cosmochim Acta 27:43–52

Davis SR, Ferry JM (1993) Fluid infiltration during contact metamorphism of interbedded marble and calc-silicate hornfels, Twin Lakes area, central Sierra Nevada, California. J Metamorphic Geol 11:71–88

deMarsily G (1986) Quantitative hydrogeology. Academic Press, San Diego

Dipple GM, Ferry JM (1992a) Fluid flow and stable isotopic alteration in rocks at elevated temperatures with applications to metamorphism. Geochim Cosmochim Acta 56:3539–3550

Dipple GM, Ferry JM (1992b) Metasomatism and fluid flow in ductile fault zones. Contrib Mineral Petrol 112:149–164

Dymoke P, Sandiford M (1992) Phase relations in Buchan facies series pelitic assemblages: calculations with application to andalusite-staurolite parageneses in the Mount Lofty Ranges, South Australia. Contrib Mineral Petrol 110:121–132

Ferry JM (1992) Regional metamorphism of the Waits River Formation: delineation of a new type of giant hydrothermal system. J Petrol 33:45–94

Ferry JM (1994) Role of fluid flow in the contact metamorphism of siliceous dolomitic limestones. Am Mineral 79:719–736

Ferry JM, Spear FS (1978) Experimental calibration of the partitioning of Fe and Mg between biotite and garnet. Contrib Mineral Petrol 66:13–117

Foden JD, Turner SP, Morrison G (1990) Tectonic implications of Delamarian magmatism in South Australia and Western Victoria. In: Jago JB, Moore PS (eds) The evolution of a late Precambrian-early Palaeozoic rift complex: the Adelaide geosyncline. Geol Soc Aust Brisbane, Spec Publ 16, pp 465–481

Friedman I, O'Neil JR (1977) Compilation of stable isotope fractionation factors of geochemical interest. US Geol Surv Washington, DC, Prof Pap 440-KK

Hanson RB (1992) Effects of fluid production on fluid flow during regional and contact metamorphism. J Metamorphic Geol 10:87–88

Hoefs J (1980) Stable isotope geochemistry, 2nd edn. Springer-Verlag, Berlin Heidelberg New York

Honma H, Sakai H (1975) Oxygen isotope study of metamorphic and granitic rocks of the Yanai district in the Ryoke belt, Japan. Contrib Mineral Petrol 52:107–112

Huang S, Bowman JR (1993) Effects of reaction kinetics and diffusion-dispersion on infiltration-driven, mixed-volatile metamorphic reactions: application of coupled heat and mass transport models (abstract). Geol Soc Am Abstr Program 25 (6):A-324

Léger A, Ferry JM (1993) Fluid infiltration and regional metamorphism of the Waits River Formation, north-east Vermont, USA. J Metamorphic Geol 11:3–30

Margaritz M, Taylor HP (1976) $^{18}O/^{16}O$ and D/H studies of igneous and sedimentary rocks along a 500 km traverse across the Coast Range Batholith into Central British Columbia at latitudes 540–550° N. Can J Earth Sci 13:1514–1536

McCrea JM (1950) On the isotope chemistry of carbonates and a paleotemperature scale. J Chem Phys 18:849–857.

Nabelek PI (1991) Stable isotope monitors. In: Kerrick DM (ed) Contact metamorphism. (Reviews in mineralogy, vol 26) Mineral Soc Am, Washington, DC, pp 395–436

Newton RC, Haselton HT (1981) Thermodynamics of the garnet-plagioclase-Al_2SiO_5-quartz geobarometer. In: Newton RC, Navrotsky A, Wood BJ (eds) Thermodynamics of minerals and melts. Springer, Berlin Heidelberg New York, pp 129–145

Norton D, Taylor HP (1979) Quantitative simulation of the hydrothermal systems of crystallizing magmas on the basis of transport theory and oxygen isotope data: an analysis of the Skaergaard intrusion. J Petrol 20:421–486

Offler R, Fleming PD (1968) A synthesis of folding and metamorphism in the Mount Lofty Ranges, South Australia. J Geol Soc Aust 15:245–266

Robie RA, Hemingway BS, Fisher JR (1978) Thermodynamic properties of minerals and related substances at 298.15 K and 1 bar (10^5 pascals) pressure and higher temperatures. US Geol Surv Bull 1452

Rumble D III (1978) Mineralogy, petrology, and oxygen isotopic geochemistry of the Clough Formation, Black Mountain, W New Hampshire, USA. J Petrol 19:317–340

Rumble D III (1994) Water circulation in metamorphism. J Geophys Res 99:15499–15502

Sandiford M, Oliver RL, Mills KJ, Allen RVA (1990) A cordierite-staurolite-muscovite association, east of Springton, Mt Lofty Ranges: implications for the metamorphic evolution of the Kanmantoo group. In: Jago JB, Moore PS (eds) The evolution of a late Precambrian-early Palaeozoic rift complex: the Adelaide geosyncline. Geol Soc Aust Brisbane, Spec Publ 16, pp 483–494

Sandiford M, Fraser G, Arnold J, Foden J, Farrow T (1995) Some causes and consequences of high-*T*, low-*P* metamorphism in the eastern Mount Lofty Ranges, South Australia. Aust J Earth Sci (in press)

Simon K, Hoefs J (1993) O, H, C isotope study of rocks from the KTB pilot hole: crustal profile and constraints on fluid evolution. Contrib Mineral Petrol 114:42–52

Stern LA, Chamberlain CP, Barnett DE, Ferry JM (1992) Stable isotope evidence for regional-scale fluid migration in a Barrovian metamorphic terrain, Vermont, USA. Contrib Mineral Petrol 112:475–489

Takasu A (1987) *P-T* histories of peridotite and amphibolite tectonic blocks in the Sanbagawa metamorphic belt, Japan. In: Daly JS, Cliff RA, Yardley BWD (eds) Evolution of metamorphic belts. Geol Soc London Spec Publ 43, pp 533–538

Taylor HP, Sheppard SMF (1986) Igneous rocks. I. Processes of isotopic fractionation and isotope systematics. In: Valley JW, Taylor HP, O'Neil JR (eds) Stable isotopes in high temperature geological processes. (Reviews in mineralogy, vol 16) Mineral Soc Am, Washington, DC, pp 227–272

Thompson AB (1982) Dehydration melting of pelitic rocks and the generation of H_2O-undersaturated granitic liquids. Am J Sci 282:1567–1595

Tracy RJ, Frost BR (1991) Phase equilibria and thermobarometry of calcareous, ultramafic and mafic rocks, and iron formations In: Kerrick DM (ed) Contact Metamorphism. (Reviews in mineralogy, vol 26) Mineral Soc Am, Washington, DC, pp 207–290

Valley JW (1986) Stable isotope geochemistry of metamorphic rocks. In: Valley JW, Taylor HP, O'Neil JR (eds) Stable Isotopes in high temperature geological processes. (Reviews in mineralogy, vol 16) Mineral Soc Am, Washington, DC, pp 445–490

Valley JW, Bohlen SR, Essene EJ, Lamb W (1990) Metamorphism in the Adirondacks. II. The role of fluids. J Petrol 35:555–596

Wickham SM (1990) Isotopic modification of the continental crust: implications for the use of isotopic tracers in granite petrogenesis. In: Ashworth JR, Brown M (eds) High-temperature metamorphism and crustal anatexis. Unwin Hyman, London, pp 124–148